NATIONAL ADVISORY COMMITTEE FOR AERONAUTICS

TECHNICAL NOTE 4031

STABILITY LIMITS AND BURNING VELOCITIES FOR SOME LAMINAR AND TURBULENT PROPANE AND HYDROGEN FLAMES AT REDUCED PRESSURE

By Burton Fine

Lewis Flight Propulsion Laboratory
Cleveland, Ohio

Washington

August 1957

NATIONAL ADVISORY COMMITTEE FOR AERONAUTICS

TECHNICAL NOTE 4031

STABILITY LIMITS AND BURNING VELOCITIES FOR SOME LAMINAR AND TURBULENT PROPANE AND HYDROGEN FLAMES AT REDUCED PRESSURE

By Burton Fine

SUMMARY

The effect of reduced pressure on blowoff, flashback, and burning velocities of propane-oxygen-nitrogen burner flames was studied (oxygen fraction of oxidant, 0.5). The pressure exponent of burning velocity, 0.22, was nearly the same as for hydrogen-air flames; stability loops showed the same blowoff and flashback characteristics as were previously observed for hydrogen-air flames. In particular, for both systems, quenching distances determined as a function of pressure from the points of intersection of flashback and blowoff portions of stability loops were considerably higher than those obtained previously by a stopped-flow method.

Of the two systems, the hydrogen-air system showed larger burning velocity, greater stability toward reduced pressure, and higher reaction order, as calculated from a simple thermal equation, and the propane-oxygen-nitrogen system showed the larger reactivity based on flashback. For both systems, laminar and turbulent flashback followed the velocity-gradient concept. However, turbulent blowoff was successfully treated by a critical boundary velocity gradient for propane-oxygen-nitrogen flames, whereas for hydrogen-air flames neither laminar nor turbulent blowoff conformed to the velocity-gradient principle.

Laminar flashback was studied for hydrogen-argon-"air" and hydrogen-helium-"air" systems over a range of pressures. These data contributed toward a general consideration of the pressure dependence of flashback for several fuel-oxidant systems. No relation was found between the critical boundary velocity gradient at 1 atmosphere and its pressure exponent. However, the critical flashback gradient at a pressure of 1 atmosphere and an equivalence ratio of 1 decreased exponentially with the reciprocal of the adiabatic flame temperature in the manner of a chemical reaction rate.

INTRODUCTION

In two previous studies stability limits and burning velocities of laminar and turbulent hydrogen-air burner flames were measured as a function of pressure (refs. 1 and 2). The present study extended the flame measurements to several other systems. The first of these was a propane-oxygen-nitrogen system in which the oxidant fraction α defined as

$$\alpha = \frac{C_{O_2}}{C_{O_2} + C_{N_2}} \qquad (1)$$

was held constant and equal to 0.50 (symbols are defined in the appendix). The other two systems investigated were hydrogen-air systems in which nitrogen was replaced by argon and helium. (In this paper hydrogen-oxygen flames with argon and helium as a diluent and with the oxygen concentration in the oxidant mixture nearly the same as for ordinary air are referred to as hydrogen-argon-"air" and hydrogen-helium-"air" flames, respectively.)

The propane-oxygen-nitrogen system was chosen for several reasons. First, the maximum burning velocity at 1 atmosphere (220 to 245 cm/sec) was fairly close to that of hydrogen-air flames (270 to 310 cm/sec). Second, laminar burning velocities had been measured at 1 atmosphere and near room temperature (311° K) by the total-area schlieren method (ref. 3). Thus, a check was available on burning velocities to be obtained at lower pressures by the same method. Furthermore, quenching distances and adiabatic flame temperatures were known over a range of subatmospheric pressures (ref. 4). Thus, it was possible to examine the effect on burner flame properties of changing the fuel and oxidant while holding burning velocity nearly constant. Generally, it was of interest to examine the extent to which relations and trends observed for hydrogen-air flames were reproduced. More specifically, it was desirable to observe whether a relation exists between chemical reactivity, as measured by the critical boundary velocity gradient for flashback, and flame stability, as measured by the approximate area within a stability loop. A final advantage of the system chosen lay in the fact that flames were intensely luminous down to the lowest pressures considered (0.058 atm), so that it was possible to observe in some detail actual flame behavior at blowoff and flashback. This was relatively difficult to observe with hydrogen flames, which are much less luminous.

The other two systems were chosen so that the effect of changing the diluent without changing fuel and oxidant might be examined. For these systems, measurements were confined to laminar flashback.

The experiments done in the present investigation and in references 1 and 2 have produced a consistent set of flashback data over a range of pressure for four fuel-oxidant systems. These data may be compared with

other results previously reported on the pressure dependence of flashback for various other systems. In the present study, the existence of two possible general relations has been considered: first, a relation between the pressure dependence of flashback and the critical boundary velocity gradient in some standard condition and, second, between some standard flashback gradient and the adiabatic flame temperature.

APPARATUS AND PROCEDURE

The apparatus used was that described in references 1 and 2; it is shown schematically in figure 1. Burner flames were established within a chamber whose pressure was regulated by a vacuum pump and a manual air bleed. The pressure within the chamber was read on a manometer. The burner itself was 50 inches long and about 3/4 inch in diameter; it was water-cooled near the lip. Tubular inserts 1.459, 1.016, 0.546, and 0.311 centimeter in diameter (about 5/8, 4/10, 1/4, and 1/8 in.) were used. The two largest inserts extended the full length of the burner. The two smallest inserts were about 2 feet long. Tank propane (chemically pure) and hydrogen (98 to 99 percent H_2) were used without further purification. Three prepared oxidant mixtures were used: 50 percent nitrogen (by volume), 50 percent oxygen; 20.6 percent oxygen, 79.4 percent argon; and 20.6 percent oxygen, 79.4 percent helium. The nominal composition of one oxidant mixture was verified by Orsat analysis. The combustible mixture was prepared by metering fuel and oxidant separately through calibrated critical-flow orifices, mixing taking place several feet upstream of the burner inlet.

For measuring stability limits, a stable flame was first established at some pressure. Then the pressure was slowly increased or decreased, at constant mass flow, until the flame flashed back or blew off. The average stream velocity at which flame loss occurred was obtained as a function of ambient pressure, burner diameter, and nominal volume flow rate at the calibration pressure (about 1 atm) by the expression

$$\bar{U}_f \text{ (or } \bar{U}_{bo}) = \frac{4V^0}{\pi D^2}\left(\frac{P^0}{P}\right) \tag{2}$$

Ambient pressures were corrected to 0° C and standard gravity. This correction was negligible for pressures greater than about 20 centimeters of mercury. Where blowoff as well as flashback data were sought, points were obtained in pairs as was done in the investigation of reference 5.

At low Reynolds numbers, near the quenching point, flames did not flashback sharply, but moved slowly back into the tube. Often this movement was asymmetric and resulted in a tilted flame (refs. 6 and 7). In this region, the flashback pressure was taken as the pressure at which a

portion of the flame first dropped below the level of the burner rim. Because of the intense luminosity of the propane flames even at the lowest pressures studied, it was possible to observe the phenomenon of "partial blowoff". At a pressure about 1 centimeter of mercury higher than the pressure at which complete blowoff occurred, a small portion of the flame base lifted from its stable position near the burner. Often this lifting was accompanied by a slow turning of the flame about a vertical axis. For hydrogen-air flames, it had not been possible to observe partial blowoff at low pressures quantitatively; hence, the criterion for blowoff had been taken as total loss of flame. For consistency, the same criterion was adopted in the present study.

Laminar burning velocities based on the total area of the schlieren cone were obtained. The pressure within the combustion chamber (accurate to about ±0.2 cm Hg) was set at a desired constant value. Flames were established above the burner port and photographed by use of a high-pressure mercury arc which gave an exposure of about 5 microseconds; composition was varied while pressure was held constant and total mass-flow rate was changed only slightly. Measurements were made at pressure levels of about 39, 19, and 12 centimeters of mercury; to avoid quenching effects (ref. 8, p. 75) burner diameter was increased as pressure was lowered. The method used for obtaining the total area of the schlieren image is described in reference 1.

Turbulent burning velocities were based on the mean surface of the visible flame brush. Measurements were made on photographic images and no correction was made for flame-front curvature. Values were obtained as described in reference 9.

BURNING VELOCITY AND STABILITY OF PROPANE-OXYGEN-NITROGEN FLAMES

Burning Velocity

Laminar burning velocities are shown in figure 2 as a function of composition at several pressures below 1 atmosphere. Also included are the data of reference 3, which were obtained in 1 atmosphere. The results for stoichiometric flames are shown cross-plotted as a function of pressure in figure 3, from which it may be seen that present results at 39 and 19 centimeters of mercury extrapolate to give previously observed values at 1 atmosphere. Values obtained at 12 centimeters of mercury were slightly higher than expected. This may have been due to the fact that, although a larger burner was used at this low pressure and measurements were made as close to flashback as was feasible, there was a considerable dead space above the rim through which a small amount of fuel-air mixture might have diverged. If this point is neglected, a pressure exponent of 0.22 is obtained at an equivalence ratio of 1. If the point were not neglected, a slightly smaller exponent would be obtained, but the difference between

the two would not be significant. Burning velocities were also cross-plotted at equivalence ratios of 0.80 and 1.20. These cross plots gave the same value for the pressure exponent as was found for $\varphi = 1.00$. Furthermore, in both cross plots data points at 12 centimeters of mercury were slightly higher than expected. As shown in figure 2, burning-velocity curves at the two lowest pressures appear to cross in the very rich region. This apparent crossing is almost certainly a result of experimental error and has no physical significance. It might be noted that, although the experimental scatter in the present results at low pressures is reasonably small, about ±5 percent, it is much larger than that found for data previously reported at 1 atmosphere. However, the previously reported data at 1 atmosphere had been subjected to a smoothing process, based on a method given in reference 10, which assumed that the flame surface was the same function of the flame base and height for all compositions and flows. No such assumption was made in the present measurements.

The value obtained for the pressure exponent of burning velocity n may be compared with that obtained for hydrogen-air flames by the same method, 0.23. From extensive measurements based on pressure rise in a constant-volume bomb, it had been concluded that mixtures having similar burning velocities at a given pressure should show about the same value for the pressure dependence (ref. 11). The two values for n given here are more than twice as large as those reported as obtained in a constant-volume bomb. However, the fact that they are nearly the same offers a limited corroboration for the proposal that chemically unlike combustible mixtures having similar burning velocities should show the same pressure dependence of burning velocity, provided that measurements for the different systems are made by the same method.

Turbulent burning velocities for stoichiometric flames are also shown in figure 3. They were obtained in a 1.016-centimeter burner at a Reynolds number of about 4000. They are discussed in connection with the mechanism of turbulent flashback.

Flashback

Flashback results for propane-oxygen-nitrogen flames are presented in figure 4 and table I. They are expressed in terms of a critical boundary velocity gradient for flashback which, in figure 4, is shown plotted logarithmically against ambient pressure. For laminar flames this critical boundary velocity gradient may be evaluated in terms of a parabolic velocity distribution to give

$$g_f = \frac{8\overline{U}_f}{D} \tag{3}$$

For turbulent flames, evaluation of the critical wall gradient is based on the fact that, for fully developed pipe turbulence, the flow in a sublayer near the wall is laminar. The relation, which depends on empirical friction data, is often expressed as (ref. 12, p. 297)

$$g_{f,t} = 0.023\ Re^{0.8}\ \frac{\overline{U}}{D} \tag{4}$$

where Reynolds number is evaluated as

$$Re = \frac{\overline{U}D\rho}{\mu} \tag{5}$$

The mixture viscosity μ was calculated by the approximation (ref. 13)

$$\mu = \frac{\sum_i \left[C_i \mu_i (M_i)^{1/2}\right]}{\sum_i \left[C_i (M_i)^{1/2}\right]} \tag{6}$$

Data are shown in figure 4 for equivalence ratios of 0.60, 0.80, 1.00, 1.25, and 1.45 and for burners 1.459, 1.016, and 0.546 centimeter in diameter. Both laminar and turbulent regimes are represented. For a given fuel-oxidant mixture there are two ranges of data points for which the critical gradient is independent of burner diameter and for which $\log g_f$ plotted against $\log P$ gives a pair of straight lines, which are nearly parallel. (An exception to this behavior is observed for the richest flames studied; there the critical boundary velocity gradient is not independent of burner diameter (see fig. 4(e)).) This and nearly all other features of flashback curves had been previously observed for hydrogen-air flames. The line which gives the lower value of g_f for any given pressure has been previously referred to as the line of normal laminar flashback. The line giving a higher value is the line of fully developed turbulent flashback. A large portion of the data for any given burner fall along these two lines. At very low Reynolds numbers, however, data for a particular burner deviate from the line of normal laminar flashback; as shown in figures 4(b), (c), and (d), the curve becomes flatter. This is the region in which flashback ceases to be a sharply explosive phenomenon. This flattening of the flashback curve has been interpreted, for hydrogen-air flames, as being caused by partial quenching of the flame by the wall (ref. 1). The explanation seems to apply equally well to the present results. Data for a given burner also deviate from the line of normal laminar flashback at some higher Reynolds number, which represents the beginning of the region of laminar-turbulent transition. In this transition region, as Reynolds number is increased flames flash back at higher values of the critical gradient, but the pressure at

flashback is nearly unchanged. The appearance of flames in this region of flashback at constant pressure confirms that laminar-turbulent transition is indeed taking place: flames are generally laminar, but display an increasing frequency of turbulent pulsations with increasing Reynolds number. Finally, at some characteristic Reynolds number, flames become steadily turbulent; data break sharply upward and follow the line of turbulent flashback with further increase in Reynolds number.

These four regions, the regions of partial quenching, normal laminar flashback, laminar-turbulent transition, and turbulent flashback, are indicated in figure 4. The extent of the transition region, that is, the crossover region from the normal laminar line to the turbulent line, is characteristic of the burner used. That is, for the 1.016- and 1.459-centimeter burners, the transition flashback region lies between Reynolds numbers of about 1500 and 2500. This range of Reynolds numbers corresponds to the transition region in cold flow, as verified by hot-wire-anemometer measurements (ref. 2). Thus, the onset of turbulence does not seem to be influenced by the presence of a flame. For the 0.546-centimeter burner, inlet conditions were unusually smooth and departure from laminar behavior was not achieved below a pressure of 1 atmosphere. As with hydrogen-air flames, critical flashback gradients in the transition region were calculated in the same way as for laminar conditions. This procedure has been justified in a previous publication (ref. 2).

It might be noted that the beginning of the transition region is characterized by an actual drop in the flashback pressure of 2 to 3 centimeters of mercury, after which the flashback pressure remains nearly constant. Reexamination of previous data shows that this initial small drop in flashback pressure had also been observed for hydrogen-air flames. No explanation for this behavior is offered at present.

Pressure exponent of flashback. - The pressure exponents for laminar and turbulent flashback are obtained from the slopes of the normal laminar and fully turbulent lines. As is true for hydrogen-air flames, the pressure exponents for laminar flashback are independent of composition over the measured range. Results for laminar flashback may be expressed as

$$\frac{\partial \log \overline{U}_f}{\partial \log P} = \frac{\partial \log g_f}{\partial \log P} = 1.13 \qquad (7)$$

where 1.13 represents an average value. Results in the turbulent region show somewhat more scatter and, perhaps, a trend toward higher values with increasing equivalence ratio. However, the average value is 1.11, about the same as for laminar flames. Since data in the laminar region are probably more accurate than the turbulent-region data, the exponent obtained for laminar flashback is used in connection with both laminar and turbulent regions. The pressure exponents of the turbulent mean stream

velocity and critical boundary velocity gradients are related, through equation (6), by the expression (ref. 2)

$$\frac{\partial \log g_{f,t}}{\partial \log P} = 0.80 + 1.8 \frac{\partial \log \bar{U}_{f,t}}{\partial \log P} \tag{8}$$

This gives a value of 0.19 for $\partial \log \bar{U}_{f,t}/\partial \log P$, in contrast with the value 0.29 observed for hydrogen-air flames.

For many fuel-oxidant systems, critical flashback gradient, laminar burning velocity, and quenching distance are related by (ref. 14)

$$g_f \propto U_b/D_q \tag{9}$$

Logarithmic differentiation of equation (9) at constant equivalence ratio gives

$$\frac{\partial \log g_f}{\partial \log P} = n - \frac{\partial \log D_q}{\partial \log P} \tag{10}$$

Hence, if combustion data for a given initial mixture are related by equation (9) over a range of pressure, corresponding pressure exponents are also related by equation (9). For the present propane-oxygen-nitrogen system, a pressure exponent for quenching distance of -0.93 has been observed at a stoichiometric fuel-oxidant ratio (ref. 4). Comparison with presently measured exponents for U_b and g_f shows that equation (9) is satisfied within experimental error. By use of present burning velocity and flashback and quenching data from reference 4, the constant of proportionality in equation (9) was evaluated for an equivalence ratio of 1. This gave, for laminar flames,

$$g_f = 3.1\ U_b/D_q \tag{11}$$

which may be compared with a coefficient of 2.6 obtained for hydrogen-air flames (ref. 1). The critical gradient is usually expressed in terms of a burning velocity and a penetration distance from the wall by the expression

$$g_f = U_b/\delta \tag{12}$$

The penetration distance δ is the smallest distance from a cold wall at which a flame can maintain the normal burning velocity U_b corresponding to a given initial mixture and ambient pressure. Thus, comparison of equations (11) and (12) shows that the coefficient 3.1 is consistent with the estimate that the quenching distance between parallel plates should be roughly twice the penetration distance (ref. 12, p. 286).

An over-all reaction order may be obtained from flashback data by a relation based on a simple thermal theory (ref. 15) and the assumption that an equation of the form of equation (9) is followed. The relation is as follows

$$\frac{\partial \log g_f}{\partial \log P} = m - 1 + \frac{E_{act}}{2R} \frac{\partial \log T_n}{\partial \log P}\left(\frac{1}{T_n} + \frac{1}{T_q}\right) \tag{13}$$

The activation energy E_{act} is taken to be 40 kilocalories per mole. This value was consistent with the value of 24 kilocalories per mole chosen for hydrogen-air flames (ref. 15). Values of T_n (2844° K) and $\partial \log T_n/\partial \log P$ (0.0252) are obtained from adiabatic flame temperatures given in reference 4 for stoichiometric mixtures. Finally, T_n is related to a quenching temperature T_q by the empirical relation (ref. 15)

$$T_q = 0.8\ T_n + 0.2\ T_o \tag{14}$$

T_q is thus found to be 2337° K at 1 atmosphere. By use of the measured average value of $\partial \log g_f/\partial \log P$, 1.13, equation (13) can be solved to give a reaction order m of 1.94. It should be noted that the last term in equation (13) represents a small correction for the pressure dependence of flame temperature, so that to a first approximation the reaction is nearly second order, and the reaction order is given by 1 plus the pressure exponent of the critical flashback gradient.

Relation between laminar and turbulent flashback. - The value of $(g_{f,t}/g_f)_p$ may be obtained directly from the lines of normal laminar and turbulent flashback shown in figure 4. Since for a given equivalence ratio these lines are not exactly parallel, probably because of experimental error, the value of $(g_{f,t}/g_f)_p$ depends slightly on pressure. Accordingly, in figure 4 values are shown at a pressure of 30 centimeters of mercury, which is approximately the pressure at which the flow becomes turbulent in the intermediate-size burner. The average value of $(g_{f,t}/g_f)_p$ is 2.8; this is in good agreement with results for hydrogen-air flames (ref. 2). In the present case, however, the value is not independent of composition, but increases with increasing equivalence ratio from 2.2 at $\varphi = 0.60$ to 3.5 at $\varphi = 1.25$. The effect of this is shown in figures 5 and 6. In figure 5, the laminar and turbulent critical gradients are plotted as functions of equivalence ratio for an ambient pressure of 30 centimeters of mercury. The laminar curve peaks at an equivalence ratio of about 1.05. The turbulent curve, however, does not appear to go through a maximum, but continues to increase rich of stoichiometric. This increase is reflected in the fact that $(g_{f,t}/g_f)_p$ increases with increasing equivalence ratio, as is shown in figure 6. This behavior with

composition is somewhat different from that shown by hydrogen-air flames for which both the laminar and turbulent critical gradients peaked at about the same equivalence ratio. Although this behavior cannot be explained at present, it may be related to other aspects of turbulent burner flames. It is well known, for example, that both turbulent burning velocity rates and space conversion rates peak considerably rich of stoichiometric for hydrocarbon-air burner flames (refs. 9 and 16).

Critical flashback gradients in the turbulent region are correlated by the relation

$$g_{f,t} = 8.7 \frac{U_b}{D_q} \quad (15)$$

where the increase in the coefficient over that given in equation (11) represents the increase in the critical gradient with turbulence. This two- or threefold increase in the critical boundary velocity gradient for flashback with turbulence has been generally observed in the past, for instance for hydrogen-isooctane-air and propane-air flames (ref. 17). Furthermore, comparison of laminar flashback data given in reference 12 (p. 293) with recent results for turbulent flames (ref. 18) shows that hydrogen-oxygen flames behave in a similar manner. Two interpretations have been offered for this generally observed increase. The first of these (ref. 17) maintains that, at flashback, a turbulent burner flame is stabilized in the turbulent portion of the boundary layer. Hence, the burning velocity governing flashback is not the laminar burning velocity, and the simple velocity gradient model cannot be applied. The alternative interpretation (ref. 2) is that a turbulent flame is stabilized in the laminar portion of the boundary layer, and that turbulent flashback is related to the velocity gradient in the laminar sublayer. If the thickness of the laminar sublayer is l centimeter, then pipe friction data indicate that at flashback the stream velocity at a distance l centimeter from the wall U_{cr} is related to the mean stream velocity by the relation (ref. 2)

$$U_{cr} = 0.75 \frac{\overline{U}_f}{Re^{0.1}} \quad (16)$$

For a pipe Reynolds number of about 5000, equation (16) becomes

$$U_{cr} = 0.3 \overline{U}_f \quad (17)$$

Since flashback is presumed to occur when the stream velocity equals the normal burning velocity at some distance δ_t from the wall, a necessary condition that a turbulent flame be stabilized in the laminar sublayer is that, at any pressure, U_{cr} at flashback exceed U_b. It had been shown that this condition was met for hydrogen-air flames at a particular pressure (ref. 2). Since the pressure exponent of the mean flashback velocity (0.29) was nearly the same as the pressure exponent of burning velocity (0.23), the relations among U_{cr}, $\overline{U}_f$, and U_b should have been nearly independent of pressure; therefore, the condition for flame stabilization in the laminar sublayer should have been met at all pressures. Furthermore, the measured increase in burning velocity due to turbulence was probably far too small to account for the increase in the critical flashback gradient. Under these conditions, then, the increase in the critical flashback gradient could be ascribed only to a decrease in the penetration distance δ with turbulence. Thus, for both hydrogen-air and propane-oxygen-nitrogen flames the relation between laminar and turbulent penetration distances may be expressed as

$$\delta_t = \left(\frac{1}{2.8}\right)\delta \tag{18}$$

Although the foregoing explanation follows naturally from experimental data, it has several weaknesses. First, it assumes that the thickness of the laminar sublayer l is accurately known and independent of the presence of a flame. Actually, the value of l is uncertain, because a large part of the boundary layer in a pipe represents a region of transition from laminar to turbulent friction. The effect of the presence of a flame is likewise unknown. Second, the validity of the observation that the pressure dependence of the mean flashback velocity is about equal to the pressure dependence of burning velocity may depend on the method used for measuring the burning velocity. That is, according to reference 11, the pressure exponent for burning velocity of hydrogen-air flames is about 0.1; this value is significantly smaller than the pressure exponent for $\overline{U}_f$ and, by equation (16), U_{cr}. Thus, according to reference 11, U_{cr} decreases more rapidly with decreasing pressure than U_b, so that at some low pressure the condition $U_{cr} > U_b$ no longer holds. A third weakness lies in the difficulty of determining the effect of a large change in an indirectly defined property, the penetration distance, on a closely related directly defined property, the dead space at the wall, which cannot be measured directly. That is, there is no adequate qualitative line of reasoning that would suggest that the dead space at the wall, as approximated by the penetration distance, should decrease markedly with turbulence. Finally, the possibility exists that the mean flame surface is not the most significant surface for determining turbulent flame speed, but that some smaller surface, perhaps the inner flame surface, is more significant. If this were so, then the turbulent burning

velocity could exceed the laminar burning velocity by an amount sufficient to account for the increase in g_f. Thus, one of the two arguments in favor of a decrease in penetration distance with turbulence would not be valid.

In any event, the laminar sublayer model appears to apply about as well to the present system as the hydrogen-air system. By equation (10), the pressure exponent of the mean stream velocity at flashback is 0.19, which is in good agreement with the presently measured value of n, 0.22. Thus, the condition $U_{cr} > U_b$ should hold at flashback. Furthermore, even if calculations based on pipe friction in cold flow are not valid, figure 3 shows that over the measured range $U_{b,t}/U_b \leq 1.4$. As with hydrogen-air flames, this increase in burning velocity is much too small to account for the increase in g_f with turbulence.

One further comparison might be made between the behavior of the present system and hydrogen-air flames. At any pressure, the critical boundary gradient for flashback is considerably higher for propane-oxygen-nitrogen flames than for hydrogen-air flames. This is true even though hydrogen-air burning velocities are slightly higher than those for propane-oxygen-nitrogen flames. The behavior of g_f does seem to follow adiabatic flame temperatures more closely, which at 1 atmosphere are 2844° K for propane-oxygen-nitrogen flames (ref. 6) and 2380° K for hydrogen-air flames (ref. 4). This correspondence is treated more extensively in a later section.

Blowoff

In figure 7 are shown the flashback and blowoff portions of stability loops at an equivalence ratio of 1 for burners 1.459, 1.016, and 0.546 centimeter in diameter. The data are given in table II. For the present system the blowoff portion as well as the flashback portion reproduces qualitatively the features displayed by the stability loops for hydrogen-air flames. In the laminar region the blowoff curve goes through a minimum; that is, there is a point on the blowoff curve where $\partial \log P / \partial \log \overline{U}_{bo}$ is zero. On the low Reynolds number side of this minimum lies the region of partial wall quenching; on the other side is the normal laminar region. As with hydrogen-air flames, the normal laminar region is not well defined; a log-log plot shows considerable curvature. Furthermore, there is no definite break in the curve corresponding to the laminar-turbulent transition region. The curves do break sharply upward, however, with the onset of fully developed turbulence. This break occurs at about the same Reynolds number for blowoff as for flashback. For the 0.546-centimeter burner, the onset of turbulence was made to occur at a lower Reynolds number by loosely packing the burner inlet with steel wool. Results are shown in figure 7(c) with and without inlet packing.

Turbulent blowoff data are adequately represented by straight lines, as shown in figure 7. Thus, the curvature shown by turbulent blowoff curves for hydrogen-air flames is not observed for the present system. Also, turbulent blowoff curves are nearly parallel to corresponding flashback curves. Finally, at any given pressure, turbulent blowoff data are nearly independent of burner diameter. That these three conditions (ref. 2) are met suggests that turbulent blowoff data may be correlated by a critical boundary velocity gradient defined as

$$g_{bo,t} = 0.023\ Re^{0.8}\ \frac{\overline{U}_{bo}}{D} \tag{19}$$

even though the corresponding gradient for laminar blowoff

$$g_{bo} = 8\ \frac{\overline{U}_{bo}}{D} \tag{20}$$

might not be satisfactory in the laminar region. The quantities g_{bo} and $g_{bo,t}$ are shown plotted as functions of pressure in figure 8. Also included are laminar data for a burner 0.311 centimeter in diameter. These critical blowoff gradients are also given in table II. Data in the region of partial wall quenching are omitted, however. The correlation in the laminar region is unsatisfactory; results are not independent of burner diameter. However, the correlation in the turbulent region is much more satisfactory. The measured slope of the line, 1.30, is reasonably close to the average slope for flashback, 1.13. For hydrogen-air flames, turbulent blowoff was not correlated by $g_{bo,t}$; blowoff curves showed a strong dependence on burner diameter. The cause of this difference in behavior is not known.

One other point of comparison may be noted. Figure 9 shows stability loops for propane-oxygen-nitrogen and hydrogen-air flames superimposed for equivalence ratios of 1.00 and 1.50 and for a 1.459-centimeter burner. For both systems the compositions chosen correspond approximately to maximum laminar reactivity (assuming g_f is a measure of flame reaction rate). Even though the propane-oxygen-nitrogen system shows a higher reactivity, since it shows a higher value of g_f for a given pressure, its over-all stability based on the area within the stability loop is less. In fact, it is less stable toward both flashback and blowoff. The difference in stability toward turbulent blowoff is particularly marked. Thus, the results show that a greater reactivity is not necessarily accompanied by greater stability toward the effect of pressure.

A portion of a stability loop for laminar stoichiometric acetylene-air flames is also shown in figure 9. Since in reference 5 no loop is given for a burner diameter of 1.459 centimeters, the present construction

is a rough estimate based on interpolation of a few characteristic points. The pressures at the quenching points and the minimums in the blowoff curves were assumed to occur at the same mean stream velocities for all burner sizes. These stream velocities were 70 and 200 centimeters per second, respectively. Log-log plots of each set of pressures against burner diameter were linear, so that values for a 1.459-centimeter burner could be obtained by interpolation. The log-log slope of the flashback curve in the normal laminar region was taken as 0.77, the value obtained in reference 5 for the 0.71-centimeter burner. The flashback curve included a region of partial quenching, which is shown by the loops in reference 5. The break in the flashback curve was made to occur at the same Reynolds number (represented by $P \times \overline{U}$ for a given burner diameter and initial mixture) as the minimum in the blowoff curve. The resulting stability loop is roughly similar to those given in reference 5 and probably is qualitatively correct. It appears, then, that acetylene-air flames having a maximum burning velocity of about 150 centimeters per second (ref. 6) are more stable toward blowoff than the other two systems considered, but, in most of the normal laminar region, show considerably less reactivity based on flashback.

Quenching Distance

It is pointed out previously that for a given burner the flashback and blowoff curves intersect at a point q (fig. 7), which gives the value of the quenching diameter for the pressure at the point of intersection (refs. 5 and 8, p. 19). If points of intersection are obtained for several burners, the quenching diameter can be plotted as a function of pressure. This has been done for several systems (ref. 8, p. 21), and most recently for the hydrogen-air system (ref. 2). In the present study the stability loops for 1.016- and 1.459-centimeter burners were closed by a reasonably short extrapolation to the point q. For the 0.546-centimeter burner the range of flows obtainable was not sufficiently large to close the loop. However, the available data give a fair estimate of the pressure at which the flashback and blowoff curves should intersect. Results are shown in figure 10 for the present system and for the hydrogen-air system. Also shown are results for the same systems as those of references 15 and 4 but obtained by a different method. In this method a stable flame was established at some pressure. The flow was then cut off, and it was carefully determined whether the flame did or did not flash back. The quenching pressure was then taken as the highest pressure at which a flame did not flash back for a given burner size. These values were corrected to give the quenching diameter. The correction factor used was the theoretical one (ref. 19). Both methods give lines which are roughly parallel and correspond to a pressure exponent of about -1. However, for both systems the method of stability loops gives considerably higher values of the quenching distance at a given pressure. The coefficients relating the critical boundary velocity gradient for flashback with the quotient U_b/D_q, 2.6 and 3.1, for hydrogen-air and propane-oxygen-nitrogen flames, respectively, were determined using data obtained by the

stopped-flow method of measuring quenching distance. If stability-loop data are used, the resulting coefficients are 4.8 and about 5.3. The value for the propane-oxygen-nitrogen system is a rough one, since quenching curves by the two methods are not exactly parallel, and the logarithmic difference is not the same at all pressures. On the basis of the simple theory that the quenching distance between parallel plates should be about twice the penetration distance defined by equation (4), the coefficients obtained by use of stopped-flow quenching data are the more reasonable.

FLASHBACK OF HYDROGEN-AIR FLAMES

In figures 11 and 12 and table III are shown critical flashback boundary velocity gradients for hydrogen-argon-"air" and hydrogen-helium-"air" flames as a function of pressure for several burners. The data are only for the normal laminar region. For hydrogen-argon-"air" flames a composition range from $\varphi = 0.90$ to $\varphi = 2.25$ is covered. For hydrogen-helium-"air" flames data are shown at equivalence ratios of 1.10 and 1.50. Results are independent of burner diameter, except for the richest mixture studied ($\varphi = 2.25$). This dependence on burner diameter was observed for the other systems studied with rich mixtures. The dependence is not consistent, however. That is, for hydrogen-air flames, the smaller burner gives a larger gradient at a given pressure. For propane-oxygen-nitrogen and hydrogen-argon-"air" flames, however, the opposite dependence is observed. Since the lines for different burners are parallel, this burner dependence does not affect the determination of the pressure exponent.

It should be first noted that flashback data for hydrogen-helium-"air" flames are almost coincident with those for hydrogen-argon-"air" flames and that both systems give, at any pressure, a value of g_f about twice as great as that observed for the hydrogen-air flames (ref. 1). At first it seems surprising that reactivity of hydrogen-helium-"air" mixtures, based on flashback, is no greater than that of hydrogen-argon-"air" mixtures, in view of the much larger burning velocity shown by helium "air" (ref. 11). However, g_f is proportional to the quotient of burning velocity divided by quenching distance; it is well known that the effect of using helium as a diluent in a combustible mixture is to increase the quenching distance and, therefore, the penetration distance as well as the burning velocity (ref. 20). Present results indicate that the two are increased by about the same amount so that by equation (12) the change in g_f is not significant. This increased quenching distance may be observed, indirectly, through the fact that the visible dead space above the rim of a hydrogen-helium-"air" flame is noticeably larger than for flames involving other diluents. The correlation of g_f with burning velocity and quenching distance has not been attempted for these systems because precise values for quenching distance at reduced pressures are not

available. Furthermore, burning velocities for helium flames are probably unreliable when obtained by a Bunsen burner method because of the extremely large dead space above the rim associated with the large quenching distance.

Adiabatic flame temperatures for hydrogen-argon-"air" and hydrogen-helium-"air" flames are the same for a given mixture at a constant pressure. This is because molar specific heats for the two diluents are identical to the degree of approximation used in calculating flame temperatures. For a stoichiometric mixture at 1 atmosphere a value of 2640° K is obtained, while 2380° K is obtained for the hydrogen-air flame. It appears, then, that within the hydrogen-oxygen-inert triad considered, there is at least a rough correspondence between g_f and the adiabatic flame temperature.

The slopes of the flashback curves give an average value for $\partial \log g_f / \partial \log P$ of 1.51 between equivalence ratios of 1.10 and 1.80. At an equivalence ratio of 0.90, the value is somewhat higher, 1.68. This is consistent with the behavior of lean hydrogen-air flames. In reference 1 a pressure exponent of 1.99 is reported for an equivalence ratio of 0.80 for hydrogen-air flames, whereas between 0.95 and 2.25 an average value of about 1.35 is reported. For the hydrogen-argon-"air" system at an equivalence ratio of 2.25, a lower value is obtained, 1.22. Since critical flashback gradients were strongly dependent on burner diameter at this equivalence ratio, the exponent obtained is probably not comparable to those obtained at leaner equivalence ratios and is not included in the average. Therefore, using the value 1.51 for the pressure exponent of flashback, one can obtain a reaction order m by equation (15). At 0.1 atmosphere the adiabatic flame temperature for a stoichiometric hydrogen-argon-"air" flame is 2477° K. Combination of this value with the value of 1 atmosphere gives $d \log T_n / d \log P = 0.029$. If an activation energy of 24 kilocalories per mole is used and the usual assumption is made relating T_n and T_q, a value of 2.37 is obtained for m. This is slightly higher than the value obtained for the hydrogen-air flame, 2.25.

Figure 13 shows a cross plot of g_f as a function of equivalence ratio at constant pressure for pressures of 76 and 30 centimeters of mercury. At an equivalence ratio of 2.25, g_f was considerably different for the two burners used. Curves are extended through data points for the larger burner in order that the two curves be similar in shape, each showing a single maximum. The maximum occurs at about 39 percent hydrogen, which agrees with the result for hydrogen-air flames. Thus, it appears that the composition of maximum reactivity is independent of the diluent.

RELATION OF FLASHBACK TO OTHER FLAME PROPERTIES

On the basis of detailed flashback results for four different fuel-oxidant systems, it becomes of interest to examine these and other flashback data available in the literature for the purpose of finding such general relations as may exist. Two possible relations are immediately suggested. The first is a relation among fuel-oxidant systems between the critical boundary velocity gradient for flashback at some reference condition and the pressure exponent for flashback. This would be analogous to the relation between burning velocity and the pressure exponent of burning velocity. Since the pressure exponent for flashback is closely related to the reaction order, such a relation would give the reaction order as an apparent function of the reaction rate. Second, if g_f does, indeed, represent a reaction rate, then some general relation should exist among fuel-oxidant systems between g_f at some reference condition and the adiabatic flame temperature, also at a reference condition.

The available data are summarized in the following table

System	T_n, °K	g_f^0, sec^{-1}	$(g_f^0)^{0.857}$	$\frac{\partial \log g_f}{\partial \log P}$	T_n Obtained from ref. -	g_f^0 Obtained from ref. -
Methane-air	2214	400	170	-----	22	12 (p. 299)
Propane-air	2253	600	240	[a]0.75	22	12 (p. 300)
Ethylene-air	2362	1,600	560	1.02	22	7
Acetylene-air	2595	5,700	1,690	.77	23	5 and 8 (p. 19)
Propane-oxygen-nitrogen	2844	15,100	3,850	1.14	22	This work
Propane-oxygen	3050	52,000	10,950	----	8 (p. 279)	12 (p. 300)
Acetylene-oxygen	3333	148,000	27,350	1.47	This work	12 (p. 294)
Hydrogen-air	2380	8,500	2,320	1.35	22	12 (p. 292)
Hydrogen-argon-"air"	2640	18,000	4,470	1.52	This work	This work
Hydrogen-helium-"air"	2640	18,000	4,470	1.50	This work	This work
Hydrogen-oxygen	3080	120,000	22,650	----	This work	12 (p. 293)
Carbon monoxide - air	2380	300	135	0.67	24	24

[a]Value for butane-air system (ref. 21).

which lists g_f for stoichiometric mixtures at a pressure of 1 atmosphere, adiabatic flame temperatures, and various values of $\partial \log g_f / \partial \log P$. In addition, values of $(g_f^0)^{0.857}$ are given, because it has been shown (ref. 14) that for very many systems U_b/D_q, the quantity proportional to a reaction rate, actually correlates with $(g_f^0)^{0.857}$. For the propane-air, propane-oxygen, and methane-air systems the values of g_f are obtained from reference 12 (pp. 299 and 300); the value of $\partial \log g_f / \partial \log P$ given for the propane-air system is actually that for the butane-air system obtained from reference 21. For the ethylene-air system entries in the table are based on flashback data given in reference 7. In that paper flashback is expressed in terms of volume flow as a function of composition at several pressures. These data were recalculated and cross-plotted to give the mean stream flashback velocity as a function of pressure, from which the log-log slope was obtained. The value of g_f at 1 atmosphere was determined by extrapolation. The entries for the acetylene-air and acetylene-oxygen systems were obtained from stability loops given in reference 3 and were based on data for a 0.71-centimeter burner. That was the largest burner for which $\log \bar{U}_f$ was linear with $\log P$ over a sufficiently long range. Again values for g_f at 1 atmosphere were obtained by a short extrapolation. Entries for carbon monoxide - air flames are based on the data given in reference 24. In that study g_f was measured at pressures from 1 to about 100 atmospheres, with the use of very carefully dried carbon monoxide; adiabatic flame temperatures were calculated over the same pressure range. The pressure exponent given in the table was obtained by cross-plotting data at several concentrations against pressure. The value found was constant over a range of concentration which included stoichiometric conditions (about 30 percent carbon monoxide) and the concentration at which g_f maximized (about 45 percent carbon monoxide). Generally, values of T_n listed are those available in the literature; for these, references are given in the table. For hydrogen-argon-"air", hydrogen-helium-"air", hydrogen-oxygen, and acetylene-oxygen systems, recent values were not readily available. For these systems T_n was calculated by the method of reference 25.

According to the table, there is no relation between g_f and its pressure exponent. In particular, the exponent for the acetylene-air system seems abnormally low. It is possible, however, that the determination of the pressure exponent is so sensitive to small errors inherent in a particular method that reliable values for the variation of the exponent could be expected only from a single set of self-consistent experimental data. Nevertheless, there appears to be a relation between g_f^0 and the adiabatic flame temperature. Figure 14 shows that when

$0.857 \log g_f^0$ is plotted against $1/T_n$, data for all five hydrocarbon systems lie on a straight line. Data for the four hydrogen-containing systems fall on a separate line whose slope is slightly less negative than that of the hydrocarbon line. If one assumes the simplest kind of relation between the reaction rate in the flame and the adiabatic flame temperature

$$\omega \propto 0.857 \ln g_f \propto e^{-E_{act}/RT_n} \tag{21}$$

then the slopes in figure 14 should give values for an activation energy. Values obtained are 66 kilocalories per mole for hydrocarbon flames and 44 kilocalories per mole for hydrogen flames. These are considerably higher than activation energies calculated either from low-temperature oxidation rates or from flame properties (refs. 22 and 23) and are probably incorrect because of the assumed extreme simplicity of the kinetics. However, the apparent hydrocarbon activation energy is considerably larger than that for hydrogen; this difference is also observed for flame activation energies obtained according to other approximations. The data point for stoichiometric carbon monoxide - air flames lies below both the hydrogen and hydrocarbon lines, which seems to indicate that carbon monoxide is less reactive than a hydrocarbon that burns at the same flame temperature. (Since the measured line-reversal temperature (ref. 12, p. 766) is very nearly the same as the calculated adiabatic temperature, this effect is not caused by a lowering of the flame temperature due to radiation.) This is also true for carbon monoxide - air flames at higher pressures. Thus, the result at 21.4 atmospheres still lies well below the hydrocarbon curve (fig. 14). By this token, then, hydrogen flames by contrast are rather more reactive than hydrocarbon flames at the same flame temperature.

SUMMARY OF RESULTS

Stability limits and burning velocities have been measured as a function of pressure for several fuel-oxidant systems. The results are summarized as follows:

1. Stability loops qualitatively reproduced features observed for hydrogen-air flames. In particular, regions of laminar-turbulent transition occurring at Reynolds numbers characteristic of cold flow in the burner were observed for both flashback and blowoff. The area within a stability loop was less, however, for the propane-oxygen-nitrogen system under corresponding conditions.

2. For laminar flashback of propane-oxygen-nitrogen flames,

$$g_f = 3.1 \frac{U_b}{D_q}$$

where g_f is the critical boundary velocity gradient, U_b is the laminar burning velocity, and D_q is the quenching distance between infinitely long parallel plates. The pressure exponent of g_f was 1.13, and at a given pressure g_f was higher than for the hydrogen-air system. Application of a thermal equation for flame propagation gave a reaction order of 1.94.

3. For propane-oxygen-nitrogen flames laminar and turbulent boundary velocity gradients at flashback were related by an expression

$$(g_{f,t}/g_f)_p = A$$

As with hydrogen-air flames A had an over-all value near 3. However, in the present case, it increased with increasing equivalence ratio.

4. For propane-oxygen-nitrogen flames laminar blowoff was not correlated satisfactorily by a critical boundary velocity gradient. However, turbulent blowoff velocity was more nearly independent of burner diameter than for hydrogen-air flames and showed about the same pressure dependence as turbulent flashback.

5. As with hydrogen-air flames, quenching distances for propane-oxygen-nitrogen flames determined from stability loops were higher than those determined by other methods.

6. For hydrogen-argon-"air" and hydrogen-helium-"air" flames a pressure dependence of 1.51 for g_f was found. Data for the two systems nearly coincided, and at any pressure gave values of g_f about twice as great as for hydrogen-air flames. A reaction order of 2.37 was calculated; the order previously obtained for hydrogen-air flames was 2.25.

7. No relation was observed among several fuel-oxidant systems between the critical boundary velocity gradient and its pressure exponent. However, for stoichiometric flames the critical boundary velocity gradient for flashback at 1 atmosphere decreased exponentially with the reciprocal of the adiabatic flame temperature, behaving, in this respect, as a chemical reaction rate.

Lewis Flight Propulsion Laboratory
National Adivsory Committee for Aeronautics
Cleveland, Ohio, May 27, 1957

APPENDIX - SYMBOLS

A	coefficient relating critical boundary velocity gradients for laminar and turbulent flashback, dimensionless
C	volume fraction, dimensionless
D	burner diameter, cm
E_{act}	activation energy, kcal/mole
g	critical boundary velocity gradient, sec^{-1}
l	thickness of laminar sublayer in turbulent pipe flow, cm
M	molar weight, g
m	reaction order, dimensionless
n	pressure exponent of burning velocity, dimensionless
P	ambient pressure, cm Hg
R	gas constant, cal/(mole)(^{o}K)
Re	Reynolds number, dimensionless
T	temperature, ^{o}K
U	velocity, cm/sec
$\overline{U}$	mean stream velocity, cm/sec
U_b	burning velocity, cm/sec
V	volume flow, cm^3/sec
α	oxidant fraction, dimensionless
δ	penetration distance, cm
μ	viscosity, poises
ρ	density, g/cm^3
φ	equivalence ratio, fuel-air ratio divided by fuel-air ratio for stoichiometric mixture

ω flame reaction rate, sec^{-1}

Subscripts:

bo blowoff

cr critical for laminar-turbulent transition

f flashback

i index of summation

n normal flame conditions

o initial conditions

p constant pressure

q quenching; D_q refers to quenching diameter or quenching distance between parallel plates, as indicated by context

t turbulent

Superscript:

0 standard conditions or calibration condition (pressure of about 1 atm and room temperature)

REFERENCES

1. Fine, Burton: Stability Limits and Burning Velocities of Laminar Hydrogen-Air Flames at Reduced Pressures. NACA TN 3833, 1956.

2. Fine, Burton: Further Experiments on the Stability of Laminar and Turbulent Hydrogen-Air Flames at Reduced Pressures. NACA TN 3977, 1957.

3. Dugger, Gordon L., and Graab, Dorothy D.: Flame Velocities of Propane- and Ethylene-Oxygen-Nitrogen Mixtures. NACA RM E52J24, 1953.

4. Berlad, Abraham L.: Flame Quenching by a Variable-Width Rectangular-Slot as a Function of Pressure for Various Propane-Oxygen-Nitrogen Mixtures. NACA RM E53K30, 1954. (See also Jour. Phys. Chem., vol. 58, no. 11, Nov. 1954, pp. 1023-1026.)

5. Wolfhard, H. G.: Die Eigenschaften stationareer Flammen im Unterdruck. Zs. f. Tech. Phys., Bd. 24, Nr. 9, 1943, pp. 206-211.

6. von Elbe, Guenther, and Mentser, Morris: Further Studies of the Structure and Stability of Burner Flames. Jour. Chem. Phys., vol. 13, no. 2, Feb. 1945, pp. 89-100.

7. Garside, J. E., Forsyth, J. S., and Townend, D. T. A.: The Stability of Burner Flames. Jour. Inst. Fuel, vol. 18, no. 103, Aug. 1945, pp. 175-185.

8. Gaydon, A. G., and Wolfhard, H. G.: Flames - Their Structure, Radiation, and Temperature. Chapman & Hall (London), 1953, p. 19.

9. Fine, Burton D., and Wagner, Paul: Space Heating Rates for Some Premixed Turbulent Propane-Air Flames. NACA TN 3277, 1956.

10. Bollinger, Lowell M., and Williams, David T.: Effect of Reynolds Number in Turbulent-Flow Range on Flame Speeds of Bunsen Burner Flames. NACA Rep. 932, 1949. (Supersedes NACA TN 1707.)

11. Manton, John, and Milliken, B. B.: Study of Pressure Dependence of Burning Velocity by the Spherical Vessel Method. Proc. Gas Dynamics Symposium (Aerothermochem.), Northwestern Univ., 1956, pp. 151-157.

12. Lewis, Bernard, and von Elbe, Guenther: Combustion, Flames and Explosion of Gases. Academic Press, Inc., 1951.

13. Rubin, Frank L.: Finding the Properties of Hydrogen Mixtures. Petr. Refiner, vol. 35, no. 3, 1956, pp. 140-149.

14. Berlad, A. L., and Potter, A. E.: Relation of Boundary Velocity Gradient for Flash-back to Burning Velocity and Quenching Distance. Combustion and Flame, vol. 1, no. 1, Mar. 1957, pp. 127-128.

15. Potter, A. E., and Berlad, A. L.: The Effect of Fuel Type and Pressure on Flame Quenching. Paper presented at Sixth Symposium (International) on Combustion, New Haven (Conn.), Aug. 19-24, 1956.

16. Wohl, Kurt, and Shore, Leon: Experiments with Butane-Air and Methane-Air Flames. Ind. and Eng. Chem., vol. 47, no. 4, Apr. 1955, pp. 828-834.

17. Wohl, Kurt: Quenching, Flash-Back, Blow-Off - Theory and Experiment. Fourth Symposium (International) on Combustion, The Williams & Wilkins Co. (Baltimore), 1953, pp. 68-89.

18. Bollinger, Loren E., and Edse, Rudolph: Effect of Burner-Tip Temperature and Flash Back of Turbulent Hydrogen-Oxygen Flames. Ind. and Eng. Chem., vol. 48, no. 4, Apr. 1956, pp. 802-807.

19. Berlad, A. L., and Potter, A. E., Jr.: Prediction of the Quenching Effect of Various Surface Geometries. Fifth Symposium (International) on Combustion, The Reinhold Pub. Corp., 1955, pp. 728-735.

20. Friedman, Raymond: The Quenching of Laminar Oxyhydrogen Flames by Solid Surfaces. Third Symposium on Combustion and Flame and Explosion Phenomena, The Williams & Wilkins Co. (Baltimore), 1949, pp. 110-120.

21. Wohl, Kurt, and Peterson, Charles: The Stability of Butane-Air Flames at Low Pressures. Meteor Rep. UAC-54, United Aircraft Corp., Feb. 1952. (Bur. Ord., Navy Dept. Contract NOrd-9845.)

22. Potter, A. E., Jr., and Berlad, A. L.: A Relation Between Burning Velocity and Quenching Distance. NACA TN 3882, 1956.

23. Fenn, John B., and Calcote, Hartwell F.: Activation Energies in High Temperature Combustion. Fourth Symposium (International) on Combustion, The Williams & Wilkins Co. (Baltimore), 1953, pp. 231-239.

24. Edse, R., and Strauss, W. A.: Stability and Burning Velocities of Laminar Carbon-Monoxide Flames at Pressures up to 93 Atmospheres. Jour. Chem. Phys., vol. 25, no. 6, 1956.

25. Huff, Vearl N., Gordon, Sanford, and Morrell, Virginia E.: General Method and Thermodynamic Tables for Computation of Equilibrium Composition and Temperature of Chemical Reactions. NACA Rep. 1037, 1951. (Supersedes NACA TN's 2113 and 2161.)

TABLE I. - FLASHBACK OF LAMINAR AND TURBULENT PROPANE-OXYGEN-NITROGEN FLAMES

[Oxidant fraction, α, 0.5]

Equivalence ratio, φ	Burner diameter, D, cm	Ambient pressure, P, cm Hg	Average flashback velocity, U_f, cm/sec	Critical boundary velocity gradient for flashback, sec^{-1}		Reynolds number, Re
				Laminar, g_f	Turbulent, $g_{f,t}$	
0.60	1.016	18.2	180	1417		307
		20.3	205	1614		391
		22.9	221	1740		474
		24.4	244	1921		559
		26.5	258	2031		641
		28.5	271	2134		722
		30.2	288	2273		814
		32.3	342	2693		1037
		35.5	363	2858		1205
		39.9	382	3008		1428
		42.8	445	3503		1783
		38.3	606	4772		2180
		39.7	692		8,396	2577
		43.1	742		10,160	2995
		48.2	750		11,260	3392
		45.9	690		9,310	2960
		51.6	695		8,319	3364
		57.5	700		10,400	3761
		65.6	675		12,000	4158
		72.1	675		12,910	4562
	1.459	12.8	160	877		276
		13.5	182	998		331
		14.6	199	1091		391
		15.5	215	1179		448
		16.3	230	1261		506
		17.2	248	1360		574
		18.7	279	1530		704
		20.5	305	1672		842
		22.1	331	1815		978
		24.2	384	2105		1250
		26.2	431	2363		1520
		26.6	503	2758		1800
		25.7	605	3317		2091
		25.4	690	3783		2361
		28.4	616		4,833	2351
		30.8	635		5,452	2631
		32.5	665		6,190	2911
		37.0	640		6,412	3191
		44.7	625		7,126	3751
		47.3	637		7,724	4051
		51.5	628		8,063	4351
		53.7	640		8,638	4631
		56.7	640		9,024	4891
		61.5	665		10,300	5501
0.80	0.546	28.4	241	3531		353
		30.3	278	4073		435
		32.6	308	4513		515
		35.0	330	4835		595
		38.1	385	5641		753
		40.9	434	6370		913
		45.0	465	6813		1074
		48.4	498	7297		1238
	1.016	14.9	194	1528		277
		15.8	211	1661		320
		17.1	247	1945		405
		17.7	289	2276		491
		19.0	318	2504		577
		20.2	336	2646		646
0.80	1.016	20.1	346	2,724		664
		23.0	385	3,031		846
		25.4	431	3,394		1048
		28.0	464	3,654		1243
		30.2	501	3,945		1450
		31.5	619	4,874		1863
		29.3	810	6,378		2268
		30.3	925		11,580	2680
		33.0	936		13,110	3085
		36.5	884		12,380	3085
		41.3	889		13,790	3505
		46.0	889		15,050	3910
		55.0	902		17,820	4742
		62.3	936		21,060	5581
		73.5	910		22,850	6398
	1.459	8.5	140	768		163
		8.9	158	866		194
		9.3	175	960		224
		9.7	213	1,168		284
		10.5	238	1,305		344
		11.4	258	1,415		404
		12.1	279	1,530		465
		12.9	298	1,634		527
		13.4	322	1,766		593
		14.8	361	1,979		754
		16.2	391	2,144		869
		17.4	427	2,341		1016
		18.7	506	2,774		1302
		20.7	557	3,054		1584
		19.3	705	3,870		1868
		19.6	800	4,390		2154
		21.9	815	4,469		2450
		22.9	870		7,708	2736
		28.1	861		8,900	3318
		31.4	903		10,820	3900
		35.2	886		11,240	4288
		39.0	895		12,430	4798
		42.1	930		14,130	5370
		46.3	936		15,450	5952
		48.5	980		17,380	6513
		57.3	974		19,650	7657
1.00	0.546	24.9	122	1,780		159
		25.3	152	2,220		201
		26.8	202	2,940		284
		28.7	244	3,575		368
		30.1	286	4,190		452
		32.1	328	4,806		538
		34.1	346	5,070		618
		37.4	414	6,050		789
		40.9	444	6,505		951
		42.5	505	7,399		1121
		45.4	521	7,634		1240
		50.2	621	9,099		1637
		55.1	705	10,330		2027
		62.2	743	10,890		2421
		64.9	827	12,120		2811
		71.5	961	14,080		3602

TABLE I. - Concluded. FLASHBACK OF LAMINAR AND TURBULENT PROPANE-OXYGEN-NITROGEN FLAMES

[Oxidant fraction, α, 0.5.]

Equivalence ratio, φ	Burner diameter, D, cm	Ambient pressure, P, cm Hg	Average flashback velocity, U_f, cm/sec	Critical boundary velocity gradient for flashback, sec^{-1}		Reynolds number, Re
				Laminar, g_f	Turbulent, $g_{f,t}$	
1.00	1.016	10.9	102	805		108
		11.4	138	1089		153
		12.5	161	1269		197
		12.9	195	1535		244
		14.2	240	1890		334
		15.4	281	2213		424
		17.6	298	2346		511
		18.4	336	2646		603
		19.5	363	2858		691
		20.7	387	3047		782
		21.9	408	3213		871
		22.4	414	3260		905
		24.0	448	3528		1048
		23.9	480	3780		1121
		25.2	545	4291		1342
		26.8	598	4693		1560
		28.4	641	5047		1777
		26.9	757	5981		1988
		26.9	838	6598		2205
		26.9	922	7260		2496
		27.6	868		9,747	2336
		28.9	983		12,570	2771
		31.9	1026		14,660	3192
		35.4	1051		16,770	3635
		38.4	1084		18,870	4062
		45.4	1110		22,740	4919
		52.4	1130		28,910	5789
		55.2	1155		28,500	6225
		58.8	1168		30,280	6660
	1.459	6.1	62	340		60
		6.5	83	455		75
		7.3	104	570		107
		7.9	125	685		138
		8.2	148	811		170
		8.6	167	916		201
		9.0	184	1009		232
		9.6	221	1212		297
		10.2	251	1376		358
		10.8	278	1524		421
		11.5	290	1590		468
		13.0	337	1848		615
		14.7	370	2029		764
		16.0	407	2232		912
		16.8	450	2467		1061
		18.2	529	2901		1349
		19.7	598	3279		1648
		18.1	769	4216		1948
		19.5	822	4507		2250
		19.5	935		7,834	2552
		20.7	985		9,026	2854
		24.7	994		10,570	3438
		27.3	965		10,860	3688
		28.1	1048		12,920	4136
		29.6	1045		13,370	4334
		31.7	1039		14,010	4626
		32.3	1095		15,660	4980
		34.2	1160		18,160	5574
		38.2	1155		19,660	6188
		42.2	1150		21,070	6782
1.25	0.546	28.0	255	3736		387
		29.9	295	4322		475
		32.3	324	4747		563
		34.4	351	5142		647
		38.0	403	5904		823
	1.016	12.1	171	1346		207
		12.9	197	1551		254
		13.5	225	1772		302
		14.3	243	1913		348
		15.4	287	2260		442
		16.7	321	2520		537
		19.9	351	2764		700
		22.5	405	3189		922
		25.1	455	3589		1143
		26.9	503	3961		1353
		28.5	558	4394		1591
		27.5	736	5795		2030
		28.2	875	6890		2469
		26.6	921		10,740	2454
		27.9	1040		13,890	2908
		30.2	1110		16,650	3361
		33.5	1140		18,950	3822
		36.3	1178		21,420	4276
		42.3	1226		25,970	5176
	1.459	7.9	127	696		145
		8.1	153	839		178
		8.5	173	949		211
		8.8	193	1058		244
		9.4	230	1261		310
		10.2	256	1404		376
		11.1	307	1683		490
		12.5	358	1963		644
		13.8	403	2210		799
		14.8	445	2440		946
		15.9	517	2835		1108
		17.4	564	3092		1410
		19.0	634	3476		1729
		17.7	798	4375		2029
		17.7	924	5066		2349
		18.3	1015		8,789	2659
		19.6	1059		10,040	2979
		22.8	1100		12,190	3620
		23.9	1160		13,880	3983
		30.3	1200		17,860	5232
		34.0	1198		19,470	5841
		34.6	1300		22,930	6471
1.45	1.016	19.7	247	1945		(a)
		23.1	309	2433		↓
		25.7	364	2866		
		28.3	411	3236		
		30.7	453	3567		
		32.4	498	3921		
		30.2	606	4772		↓
	1.459	12.8	271	1486		(a)
		13.9	328	1798		↓
		15.8	360	1974		
		16.9	400	2193		
		17.8	441	2418		
		18.7	479	2626		
		19.9	505	2769		↓

[a]No values of Re were computed, since all flames were in normal laminar region.

TABLE II. - BLOWOFF OF LAMINAR AND TURBULENT PROPANE-OXYGEN-NITROGEN FLAMES

[Equivalence ratio, φ, 1.00; oxidant fraction, α, 0.5.]

Burner diameter, D, cm	Ambient pressure, P, cm Hg	Average blowoff velocity, $\bar{U}_{bo}$, cm/sec	Critical boundary velocity gradient for blowoff, sec^{-1}	
			Laminar, g_{bo}	Turbulent, $g_{bo,t}$
0.311	19.0	913	23,490	
	19.7	1133	29,140	
	21.1	1308	33,050	
	22.8	1432	36,830	
	24.3	1550	39,870	
	25.6	1880	48,360	
	28.3	2050	52,730	
	30.9	2213	56,920	
	32.7	2320	59,680	
	35.8	2785	71,640	
	39.3	3140	80,770	
0.546	8.4	361	4,980	
	8.4	456	6,681	
	8.7	623	9,128	
	9.0	775	11,350	
	9.3	917	13,440	
	10.1	1016	14,890	
	10.9	1082	15,850	
	11.6	1300	19,050	
	12.6	1440	21,100	
	13.2	1620	23,740	
	13.3	1780	26,080	
	15.1	2055	30,110	
	16.7	2310	33,850	
	17.7	2610	38,240	
	19.7	2720	39,850	
	22.2	3090	45,270	
	26.3	3180	46,590	
	27.5	3600	52,750	
	33.7	2350	34,430	
0.546	50.4	2550	37,360	
	60.5	2330		118,700
	64.0	2370		126,300
	70.7	2260		131,400
[a]0.546	24.1	2190		51,840
	30.6	2220		64,610
	36.6	2290		78,610
	41.6	2370		92,530
	47.4	2400		106,100
	53.9	2390		115,800
	58.4	2470		131,600
	63.9	2480		144,200
1.016	7.4	149	(b)	
	7.1	221	↓	
	6.8	296		
	6.0	418		
	5.9	580	4,567	
	6.2	700	5,512	
	6.3	833	6,559	
	6.5	950	7,480	
	6.9	1026	8,079	
	7.4	1080	8,504	
	7.8	1142	8,992	
	8.2	1130	8,898	
	8.2	1310	10,310	
	9.1	1262	9,937	
	9.5	1450	11,420	
	9.9	1614	12,710	
	10.6	1716	13,510	
	11.3	1805	14,210	

[a]With packed inlet.

[b]Partially quenched; not shown in fig. 8.

TABLE II. - Concluded. BLOWOFF OF LAMINAR AND TURBULENT PROPANE-OXYGEN-NITROGEN FLAMES

[Equivalence ratio, φ, 1.00; oxidant fraction, α, 0.5.]

Burner diameter, D, cm	Ambient pressure, P, cm Hg	Average blowoff velocity, $\bar{U}_{bo}$, cm/sec	Critical boundary velocity gradient for blowoff, sec^{-1}		Burner diameter, D, cm	Ambient pressure, P, cm Hg	Average blowoff velocity, $\bar{U}_{bo}$, cm/sec	Critical boundary velocity gradient for blowoff, sec^{-1}	
			Laminar, g_{bo}	Turbulent, $g_{bo,t}$				Laminar, g_{bo}	Turbulent, $g_{bo,t}$
1.016	13.7	1745		19,590	1.459	4.7	710	3,893	
	13.9	1785		21,010		5.1	860	4,716	
	15.4	1840		23,330		5.5	990	5,428	
	17.4	1876		26,970		5.8	1024	5,615	
	19.1	1950		31,080		6.0	1259	6,903	
	20.2	2060		35,910		6.4	1505	8,252	
	22.7	2220		45,230		6.8	1730	9,480	
	27.4	2160		49,880		7.5	1850	10,140	
	28.9	2200		53,790		8.8	1820	9,980	
	31.2	2180		56,510		10.5	1736		14,500
1.459	4.6	93	(a)			11.8	1725		15,790
	4.5	119	↓			13.6	1800		19,200
	4.4	173				15.3	1929		23,770
	4.4	224				14.6	1800		20,170
	4.4	275				16.6	1800		23,890
	4.5	319				17.7	1860		25,060
	4.7	353	↓			18.6	1905		27,170
	4.6	460	2,522			20.9	1900		29,490
	4.6	563	3,087			21.7	2030		34,550
	4.8	627	3,438			23.3	2080		37,860

[a] Partially quenched; not shown in fig. 8.

TABLE III. - FLASHBACK OF LAMINAR HYDROGEN-AIR FLAMES

(a) Diluent, argon

Equivalence ratio, φ	Burner diameter, D, cm	Ambient pressure, P, cm Hg	Average flashback velocity, $\bar{U}_f$, cm/sec	Critical boundary velocity gradient for laminar flashback, g_f, sec^{-1}	Equivalence ratio, φ	Burner diameter, D, cm	Ambient pressure, P, cm Hg	Average flashback velocity, $\bar{U}_f$, cm/sec	Critical boundary velocity gradient for laminar flashback, g_f, sec^{-1}
0.90	0.546	39.1	330	4,834	1.10	1.016	19.0	266	2,091
		41.8	349	5,113			20.7	296	2,327
		43.1	380	5,567			22.0	327	2,575
		46.3	429	6,285			22.9	359	2,827
		49.3	473	6,929			23.1	368	2,898
		51.5	519	7,603			25.6	429	3,378
		51.1	540	7,911			28.5	474	3,732
		55.6	641	9,390			30.9	519	4,087
		59.8	732	10,720			32.6	568	4,472
		63.1	824	12,070			34.8	675	5,315
		70.4	853	12,500			32.5	877	6,905
	1.016	18.5	175	1,378	1.50	0.546	29.9	307	4,498
		19.6	190	1,496			31.4	357	5,230
		20.3	208	1,638			33.6	395	5,787
		20.8	227	1,787			36.0	426	6,241
		22.1	259	2,043			39.1	498	7,296
		23.6	286	2,252			42.1	560	8,204
		24.9	306	2,409			45.1	615	9,010
		24.8	310	2,441			48.7	674	9,874
		27.1	380	2,992			53.2	799	11,700
		30.1	421	3,315			57.5	905	13,260
		32.0	476	3,748			62.0	996	14,590
		34.1	509	4,008			65.6	1085	15,890
		36.7	600	4,724		1.016	17.1	259	2.039
		34.0	785	6,181			18.4	306	2,409
1.10	0.546	31.8	258	3,780			20.0	341	2,685
		32.5	310	4,542			21.5	373	2,937
		34.4	347	5,084			22.8	404	3,181
		36.0	383	5,612			23.1	410	3,228
		40.0	437	6,403			25.6	479	3,772
		41.8	506	7,414			27.9	538	4,236
		44.8	556	8,147			29.9	596	4,693
		47.1	605	8,864			31.8	647	5,094
		47.7	617	9,040			34.5	760	5,984
		51.4	739	10,830			33.3	953	7,504
		56.6	825	12,090					

TABLE III. - Continued. FLASHBACK OF LAMINAR HYDROGEN-AIR FLAMES

(a) Concluded. Diluent, argon

Equivalence ratio, φ	Burner diameter, D, cm	Ambient pressure, P, cm Hg	Average flashback velocity, U_f, cm/sec	Critical boundary velocity gradient for laminar flashback, g_f, sec^{-1}	Equivalence ratio, φ	Burner diameter, D, cm	Ambient pressure, P, cm Hg	Average flashback velocity, U_f, cm/sec	Critical boundary velocity gradient for laminar flashback, g_f, sec^{-1}
1.80	0.546	28.0	274	4,014	2.25	0.546	36.7	365	5,347
		30.1	328	4,805			42.1	434	6,358
		32.4	374	5,479			47.1	493	7,222
		34.6	414	6,065			51.6	545	7,984
		36.5	453	6,636			60.6	646	9,464
		40.6	517	7,574			66.0	766	11,130
		44.4	573	8,394		1.016	17.1	227	2,788
		47.7	625	9,156			18.7	247	3,041
		51.0	671	9,830			19.7	269	3,305
		51.5	686	10,050			21.9	306	3,767
		57.2	800	11,720			23.8	341	4,198
		62.4	897	13,140			25.7	371	4,567
		66.4	1010	14,800			27.5	412	5,072
		70.4	1093	16,010			31.1	471	5,798
	1.016	16.8	246	1,937			34.4	522	6,426
		17.7	270	2,126			37.1	573	7,657
		19.6	309	2,433			39.6	622	7,054
		21.1	349	2,748					
		22.7	380	3,039					
		25.7	398	3,134					
		27.6	478	3,764					
		29.9	544	4,283					
		32.4	594	4,677					
		33.9	655	5,157					
		37.4	754	5,937					

TABLE III. - Concluded. FLASHBACK OF LAMINAR HYDROGEN-AIR FLAMES

(b) Diluent, helium.

Equivalence ratio, φ	Burner diameter, D, cm	Ambient pressure, P, cm Hg	Average flashback velocity, $\bar{U}_f$, cm/sec	Critical boundary velocity gradient for laminar flashback, g_f, sec^{-1}	Equivalence ratio, φ	Burner diameter, D, cm	Ambient pressure, P, cm Hg	Average flashback velocity, $\bar{U}_f$, cm/sec	Critical boundary velocity gradient for laminar flashback, g_f, sec^{-1}
1.10	0.546	35.9	335	4,908	1.50	0.546	35.0	383	5,611
		39.7	399	5,845			38.6	458	6,710
		41.9	468	6,856			41.7	525	7,691
		44.7	524	7,677			44.4	588	8,614
		47.9	568	8,321			47.4	642	9,406
		50.6	614	8,995			50.3	685	10,040
		52.7	660	9,669			52.9	735	10,770
		57.4	740	10,840			57.9	817	11,970
		61.7	810	11,870			62.9	885	12,970
		64.8	894	13,100					
	1.016	19.4	235	1,850		1.016	19.2	266	2,094
		20.7	274	2,157			20.6	308	2,425
		21.8	311	2,449			21.9	345	2,717
		22.9	344	2,709			23.1	381	3,000
		24.0	374	2,945			24.2	412	3,244
		25.6	403	3,173			25.3	433	3,409
		27.3	450	3,543			27.5	496	3,906
		29.2	495	3,898			29.7	541	4,260
		31.2	535	4,213			32.1	578	4,551
		32.9	575	4,528			33.5	626	4,929

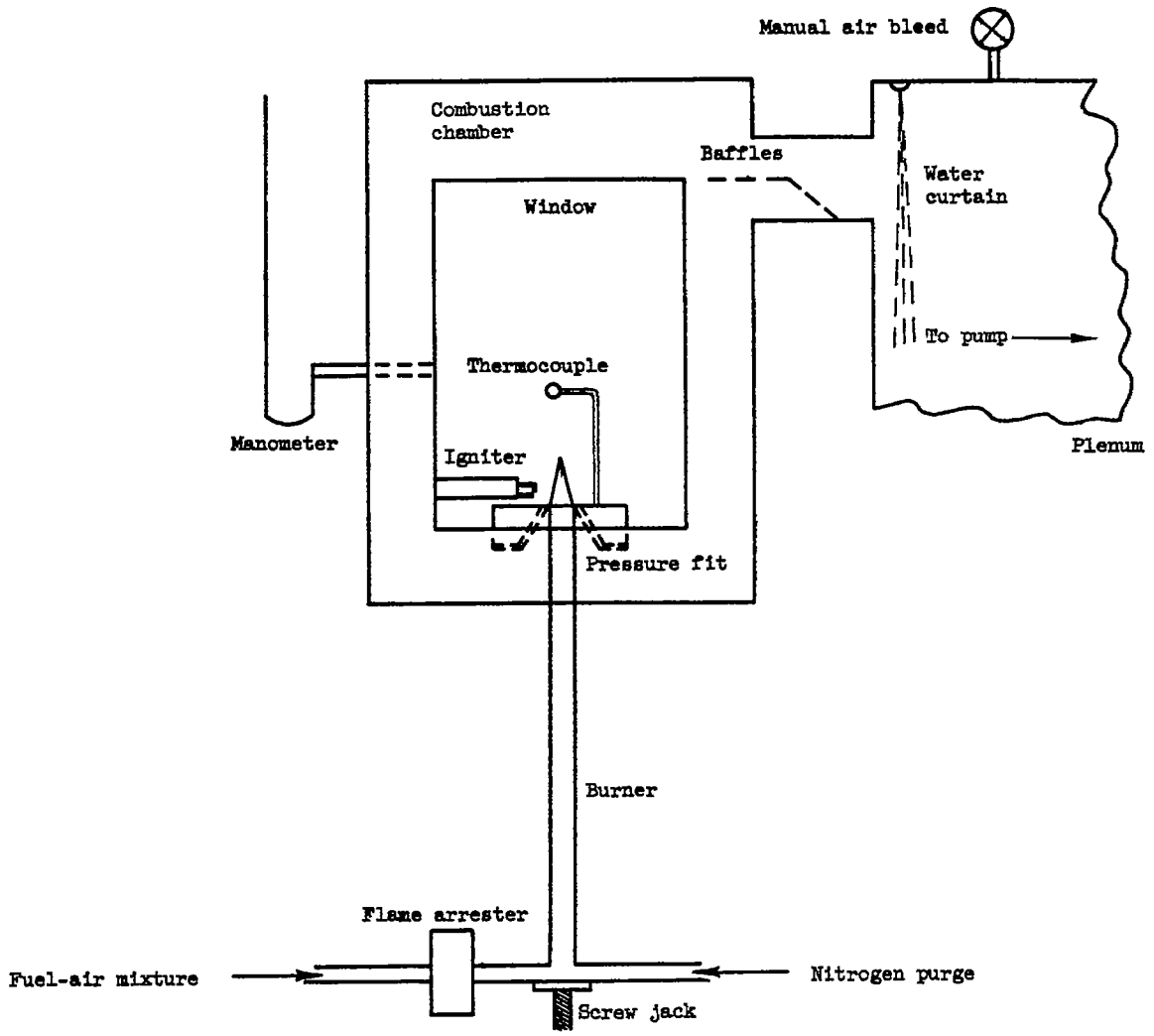

Figure 1. - Combustion apparatus.

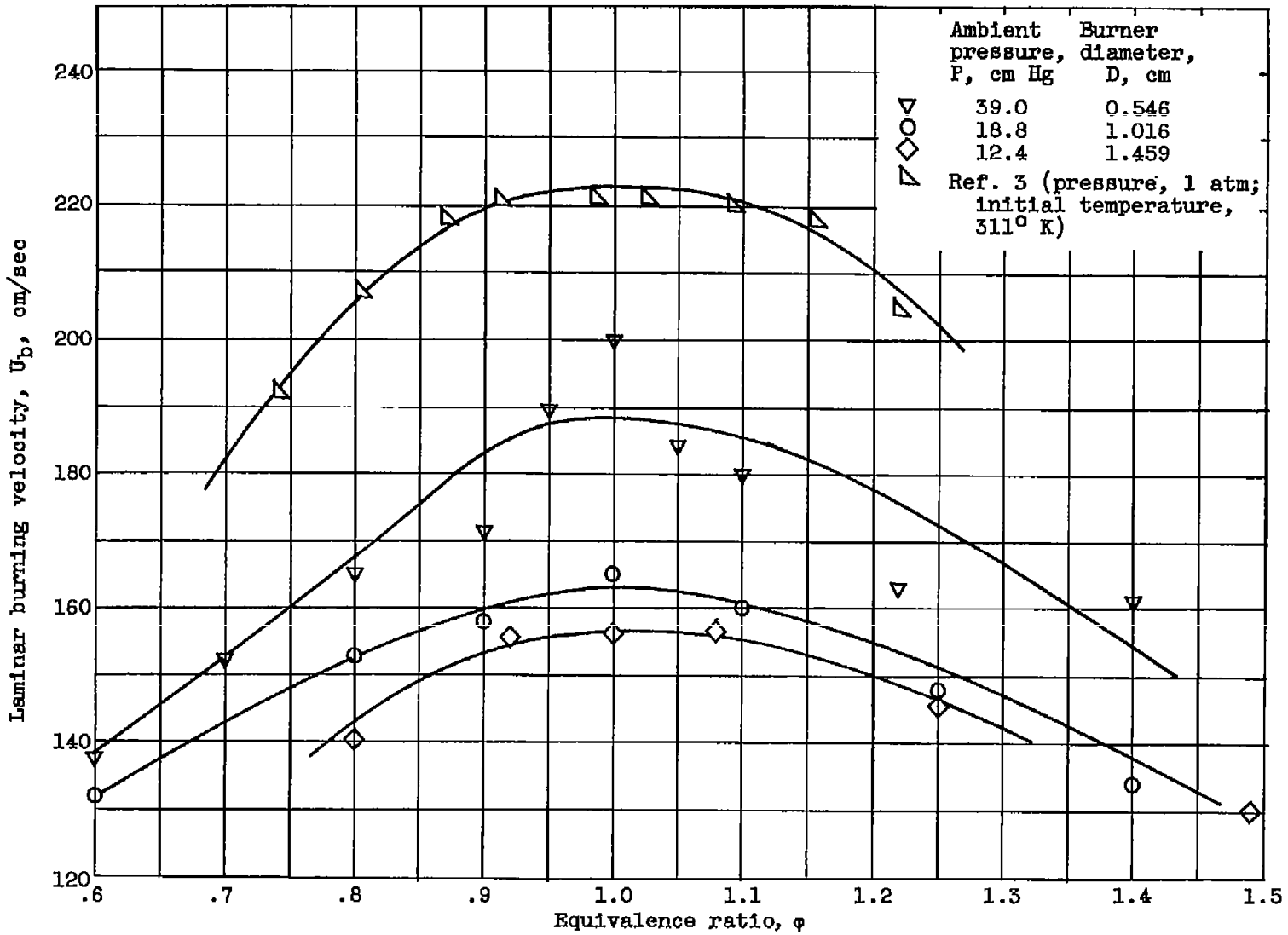

Figure 2. - Burning velocity as function of equivalence ratio at various pressures for propane-oxygen-nitrogen flames.

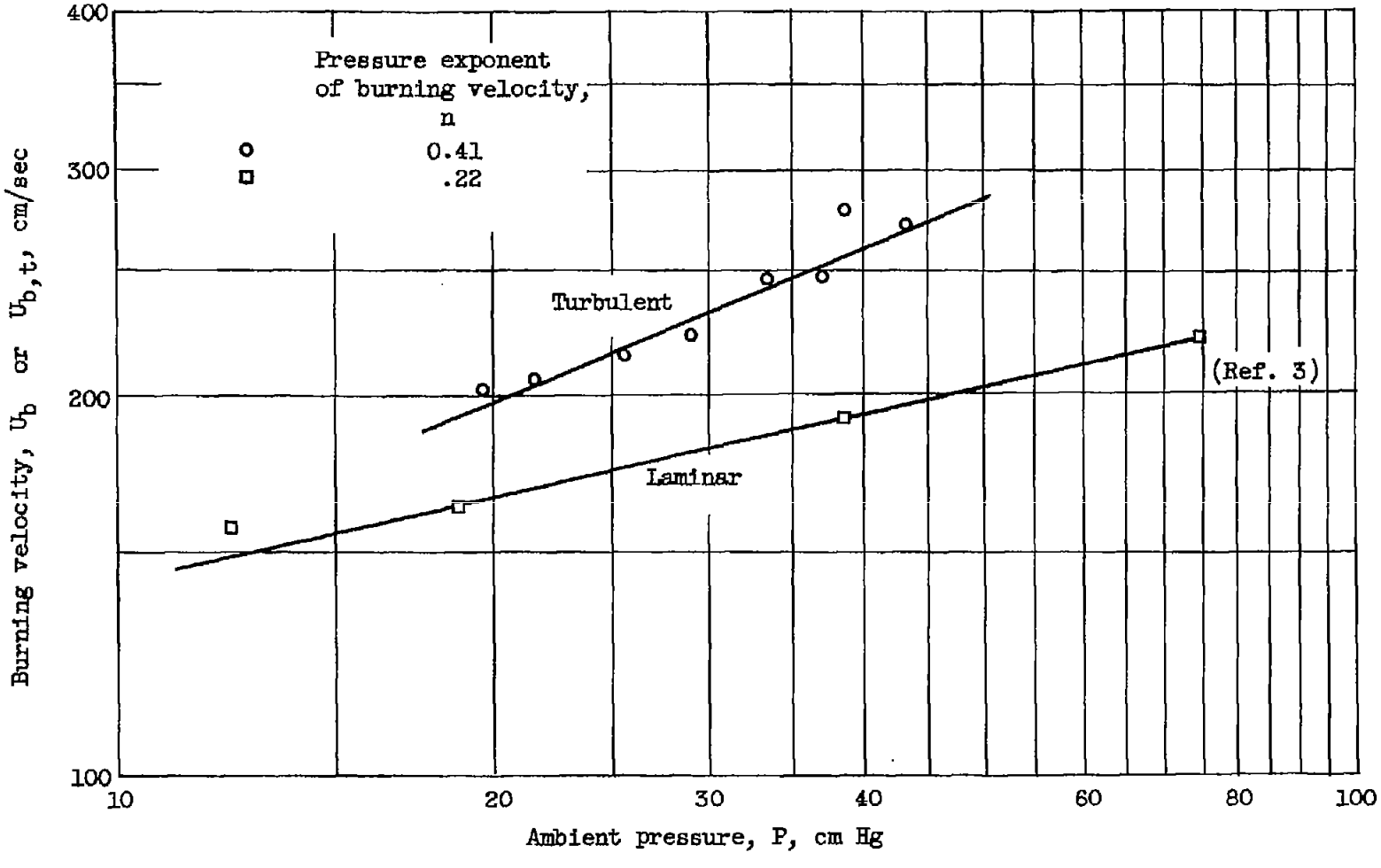

Figure 3. - Pressure dependence of burning velocity for propane-oxygen-nitrogen flames. Equivalence ratio, 1.00; oxygen fraction of oxidant, 0.5.

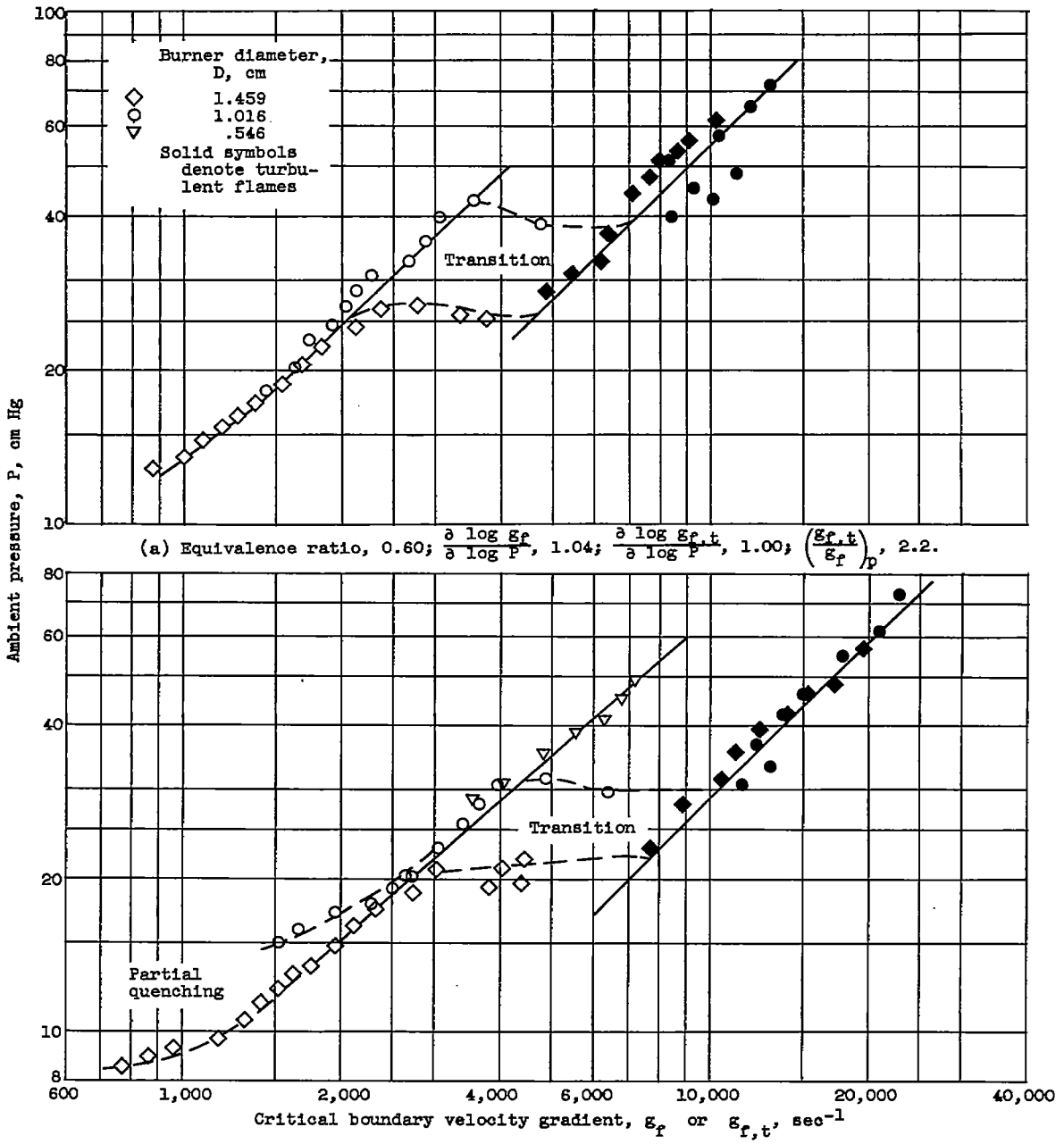

(a) Equivalence ratio, 0.60; $\frac{\partial \log g_f}{\partial \log P}$, 1.04; $\frac{\partial \log g_{f,t}}{\partial \log P}$, 1.00; $\left(\frac{g_{f,t}}{g_f}\right)_p$, 2.2.

(b) Equivalence ratio, 0.80; $\frac{\partial \log g_f}{\partial \log P}$, 1.10; $\frac{\partial \log g_{f,t}}{\partial \log P}$, 0.98; $\left(\frac{g_{f,t}}{g_f}\right)_p$, 2.42.

Figure 4. - Flashback of propane-oxygen-nitrogen flames. Oxygen fraction of oxidant, 0.5.

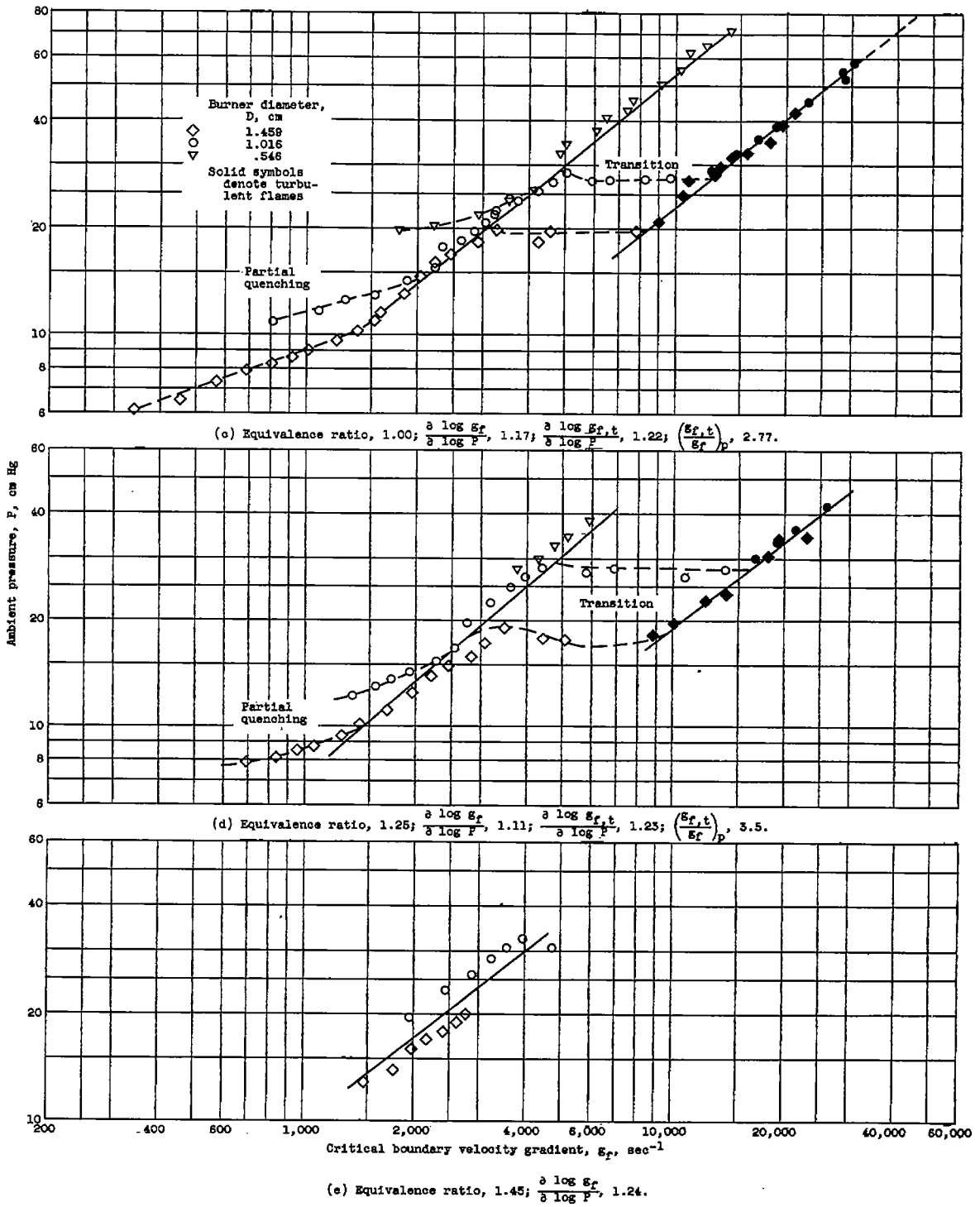

(a) Equivalence ratio, 1.00; $\frac{\partial \log g_f}{\partial \log P}$, 1.17; $\frac{\partial \log g_{f,t}}{\partial \log P}$, 1.22; $\left(\frac{g_{f,t}}{g_f}\right)_p$, 2.77.

(d) Equivalence ratio, 1.25; $\frac{\partial \log g_f}{\partial \log P}$, 1.11; $\frac{\partial \log g_{f,t}}{\partial \log P}$, 1.23; $\left(\frac{g_{f,t}}{g_f}\right)_p$, 3.5.

(e) Equivalence ratio, 1.45; $\frac{\partial \log g_f}{\partial \log P}$, 1.24.

Figure 4. - Concluded. Flashback of propane-oxygen-nitrogen flames. Oxygen fraction of oxidant, 0.5.

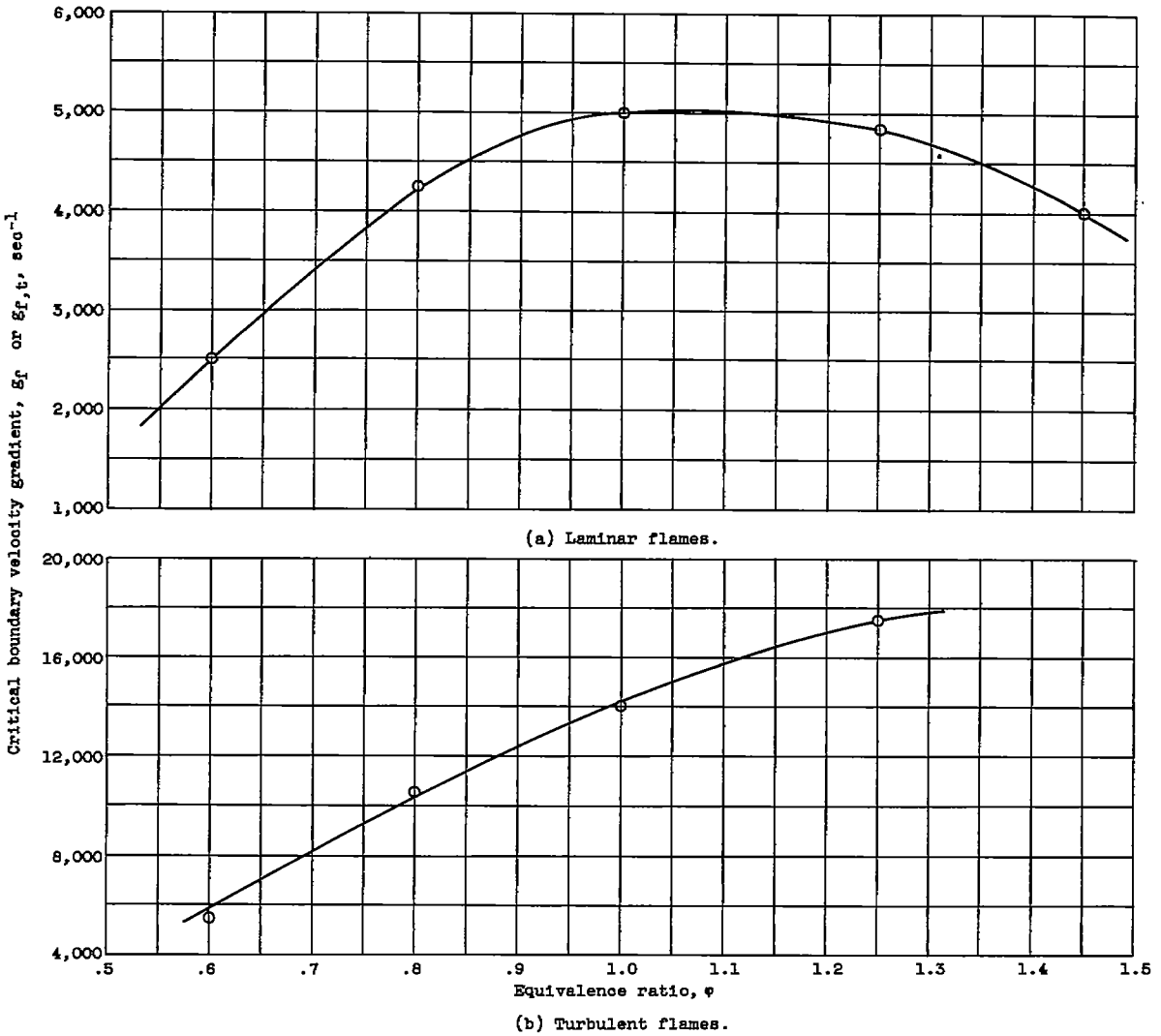

Figure 5. - Flashback critical boundary velocity gradient as function of equivalence ratio for propane-oxygen-nitrogen flames. Ambient pressure, 30 centimeters of mercury.

Figure 6. - Coefficient relating critical boundary velocity gradients as function of equivalence ratio.

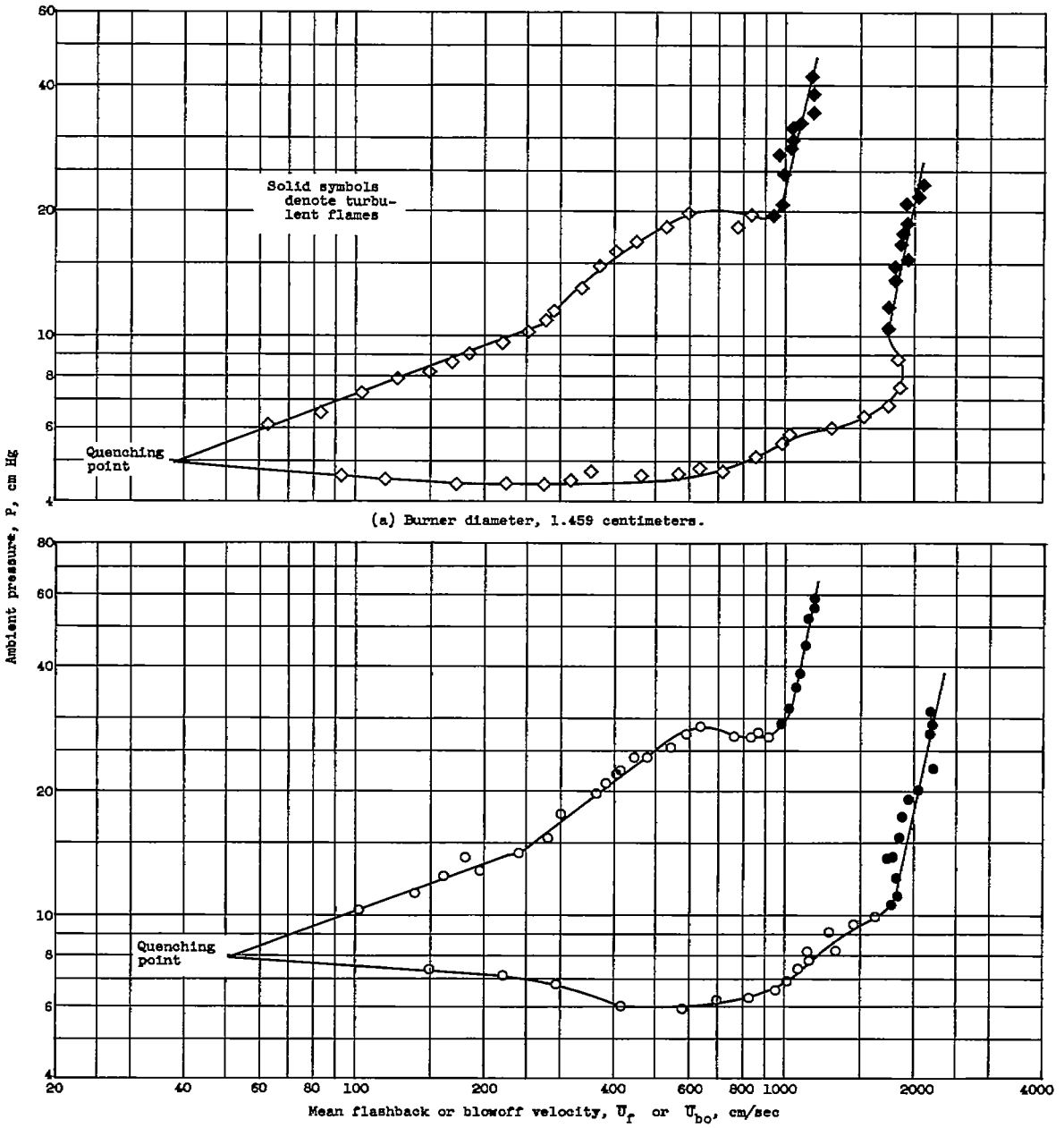

(a) Burner diameter, 1.459 centimeters.

(b) Burner diameter, 1.016 centimeters.

Figure 7. - Stability loops for propane-oxygen-nitrogen flames. Equivalence ratio, 1.00; oxygen fraction of oxidant, 0.5.

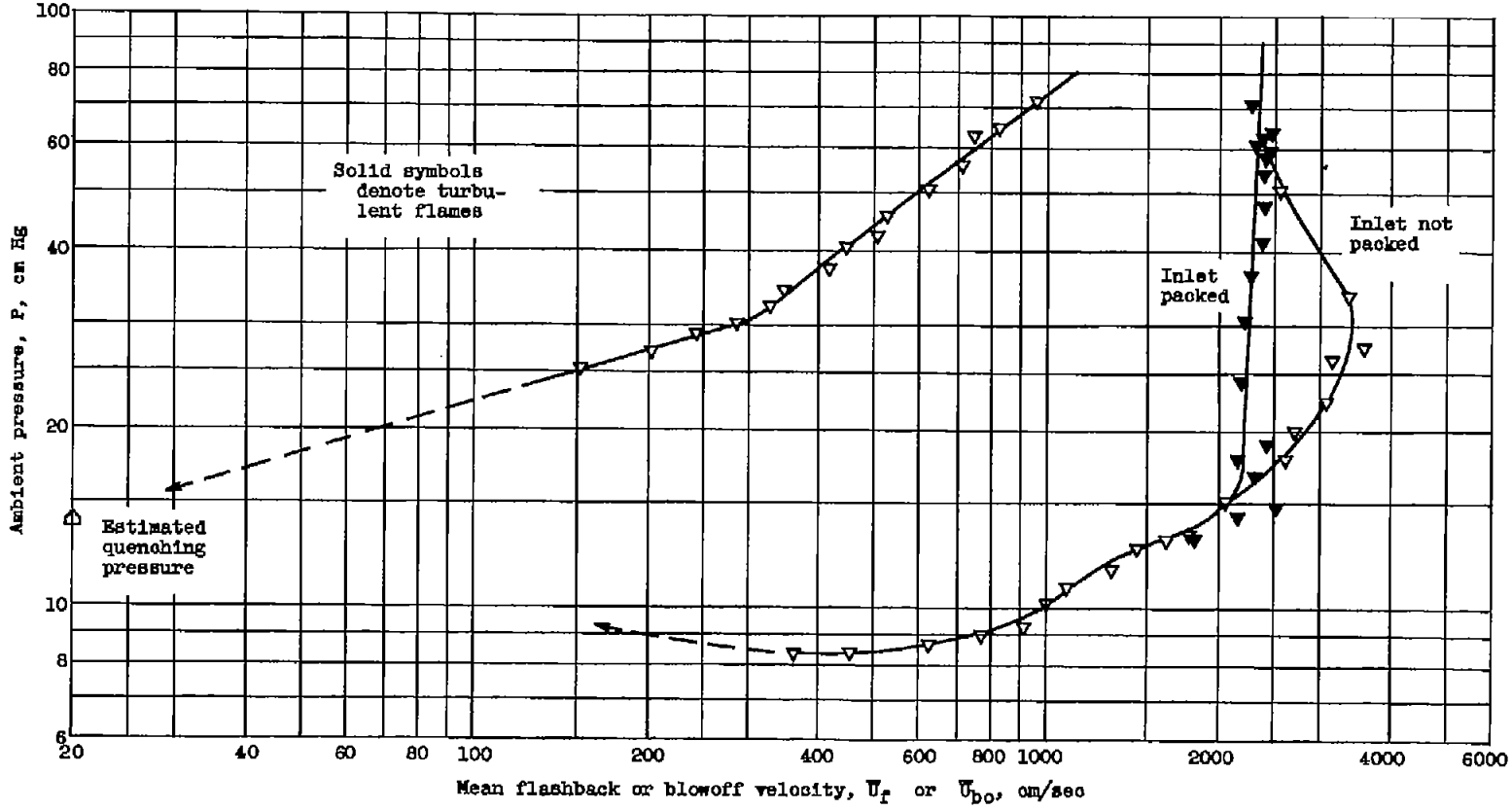

(c) Burner diameter, 0.546 centimeter.

Figure 7. - Concluded. Stability loops for propane-oxygen-nitrogen flames. Equivalence ratio, 1.00; oxygen fraction of oxidant, 0.5.

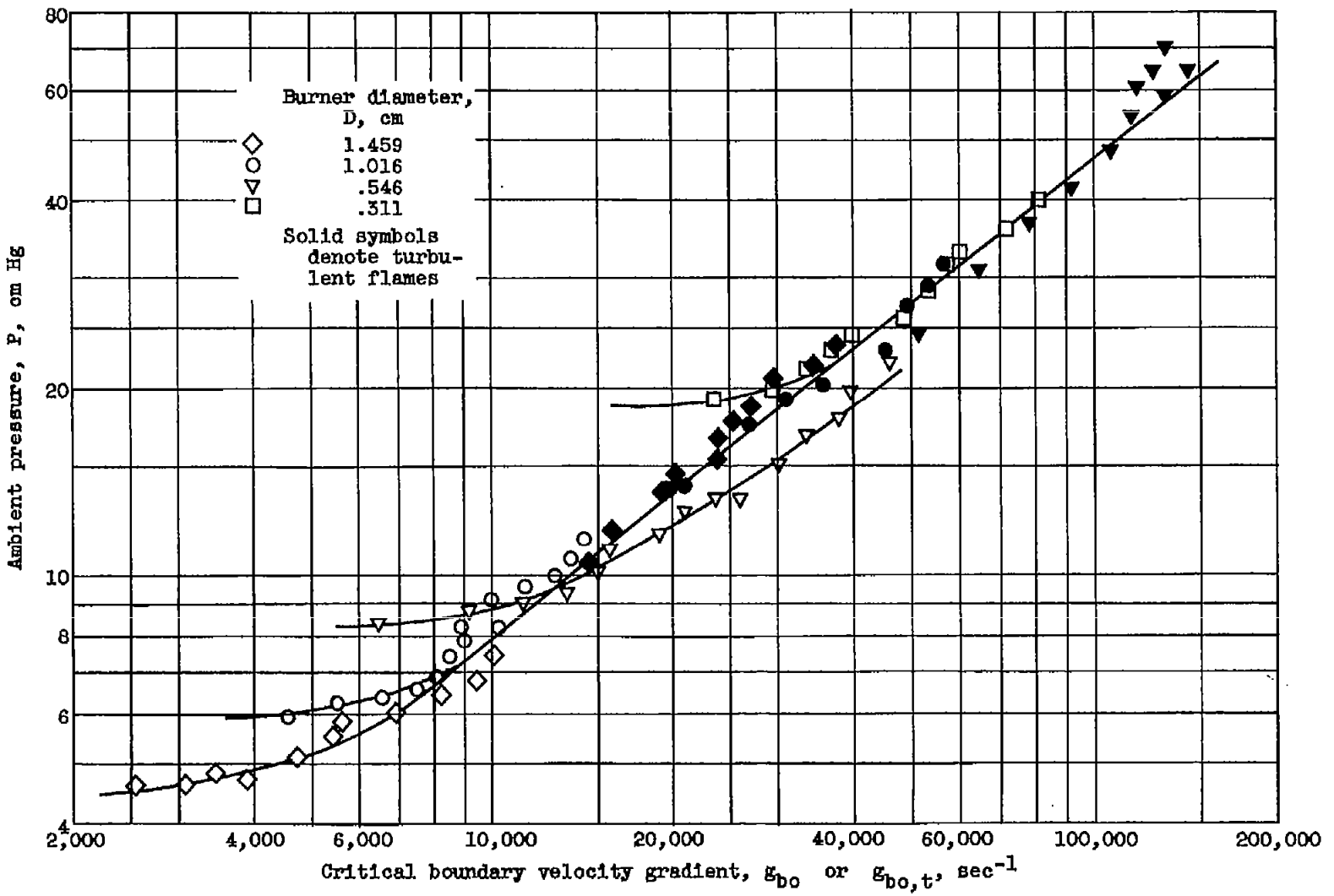

Figure 8. - Blowoff of propane-oxygen-nitrogen flames. Equivalence ratio, 1.00; oxygen fraction of oxidant, 0.5; $\frac{\partial \log g_{bo,t}}{\partial \log P}$, 1.30.

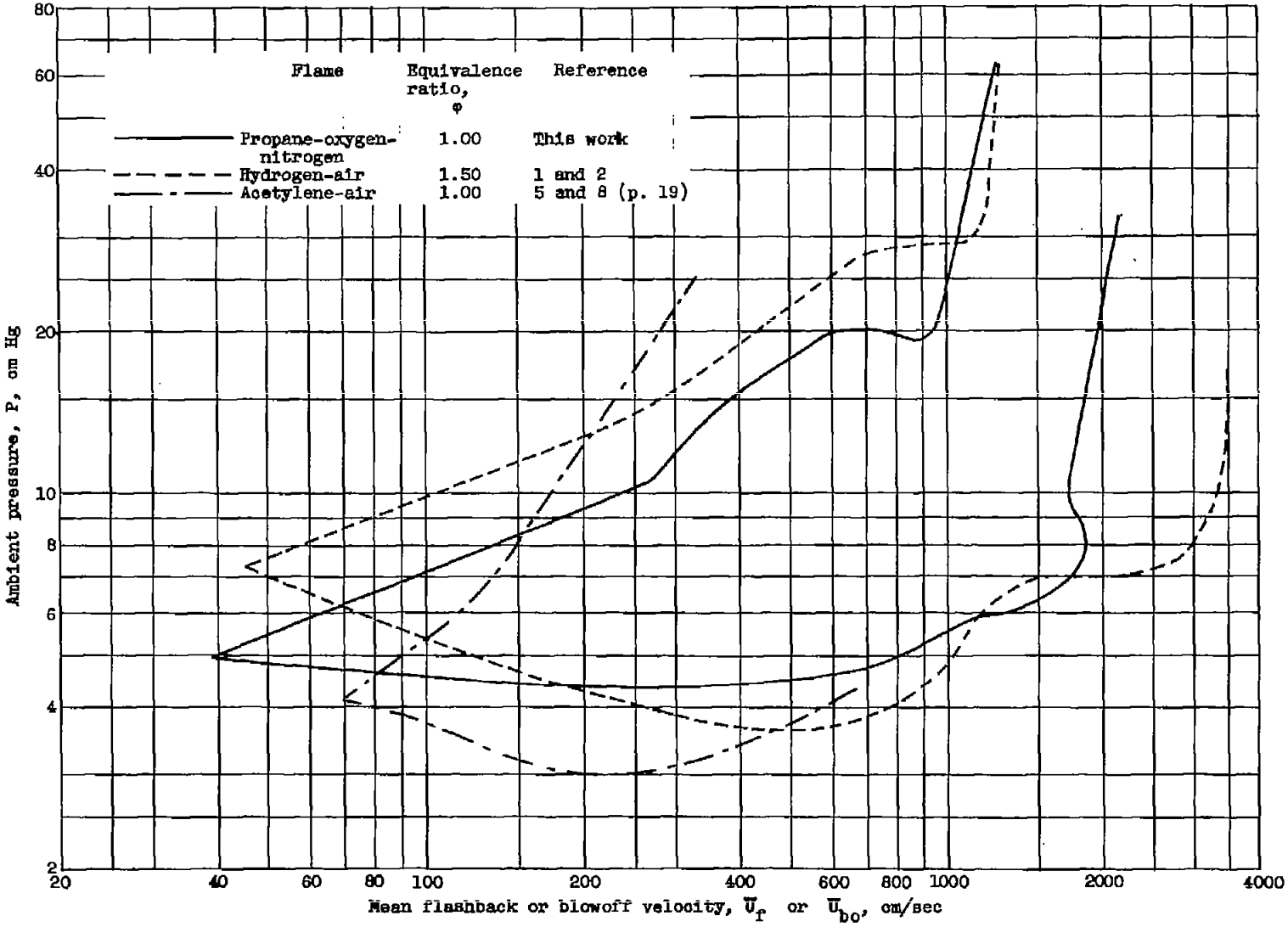

Figure 9. - Comparison of stability loops. Burner diameter, 1.459 centimeters.

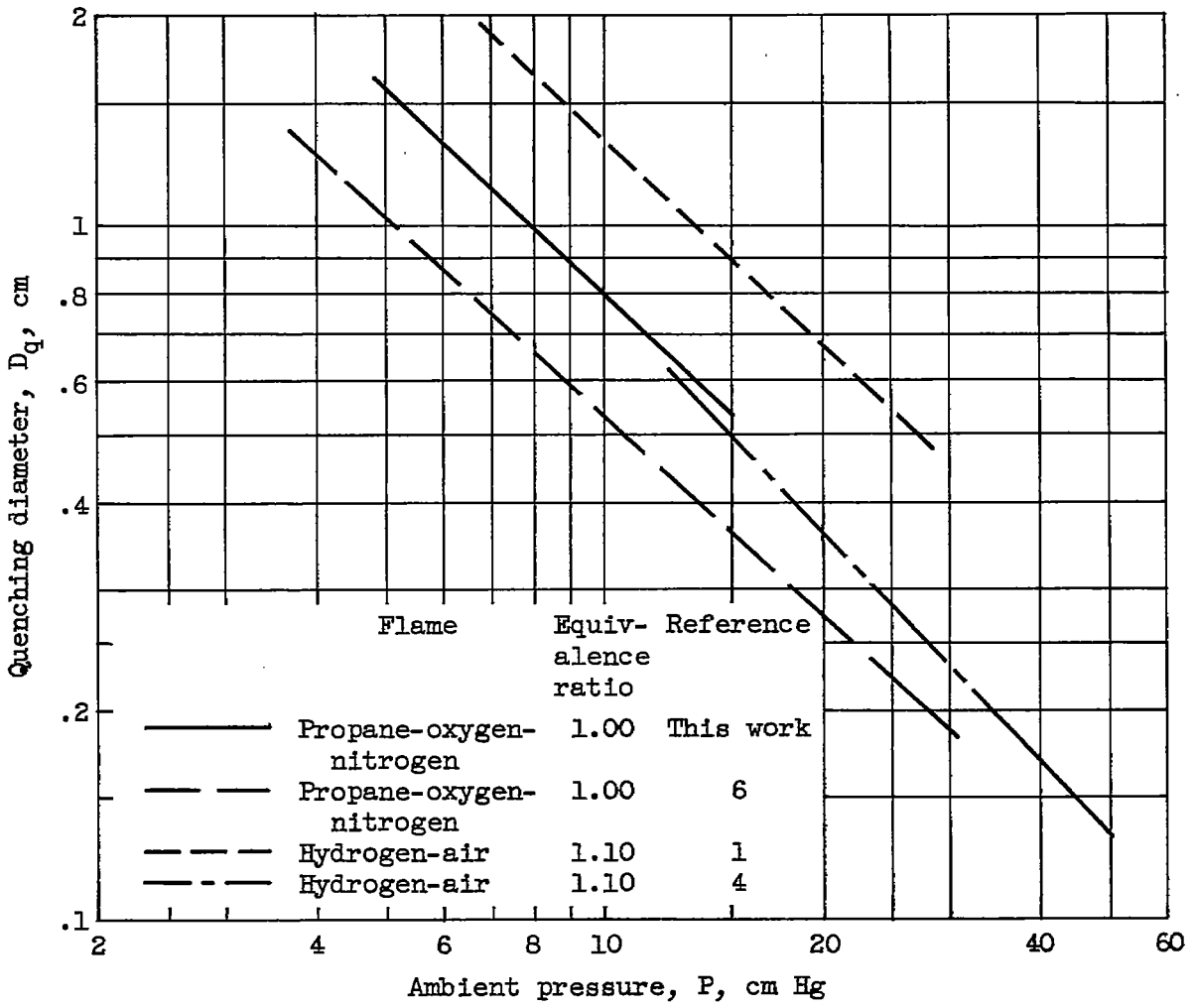

Figure 10. - Quenching diameter as function of pressure.

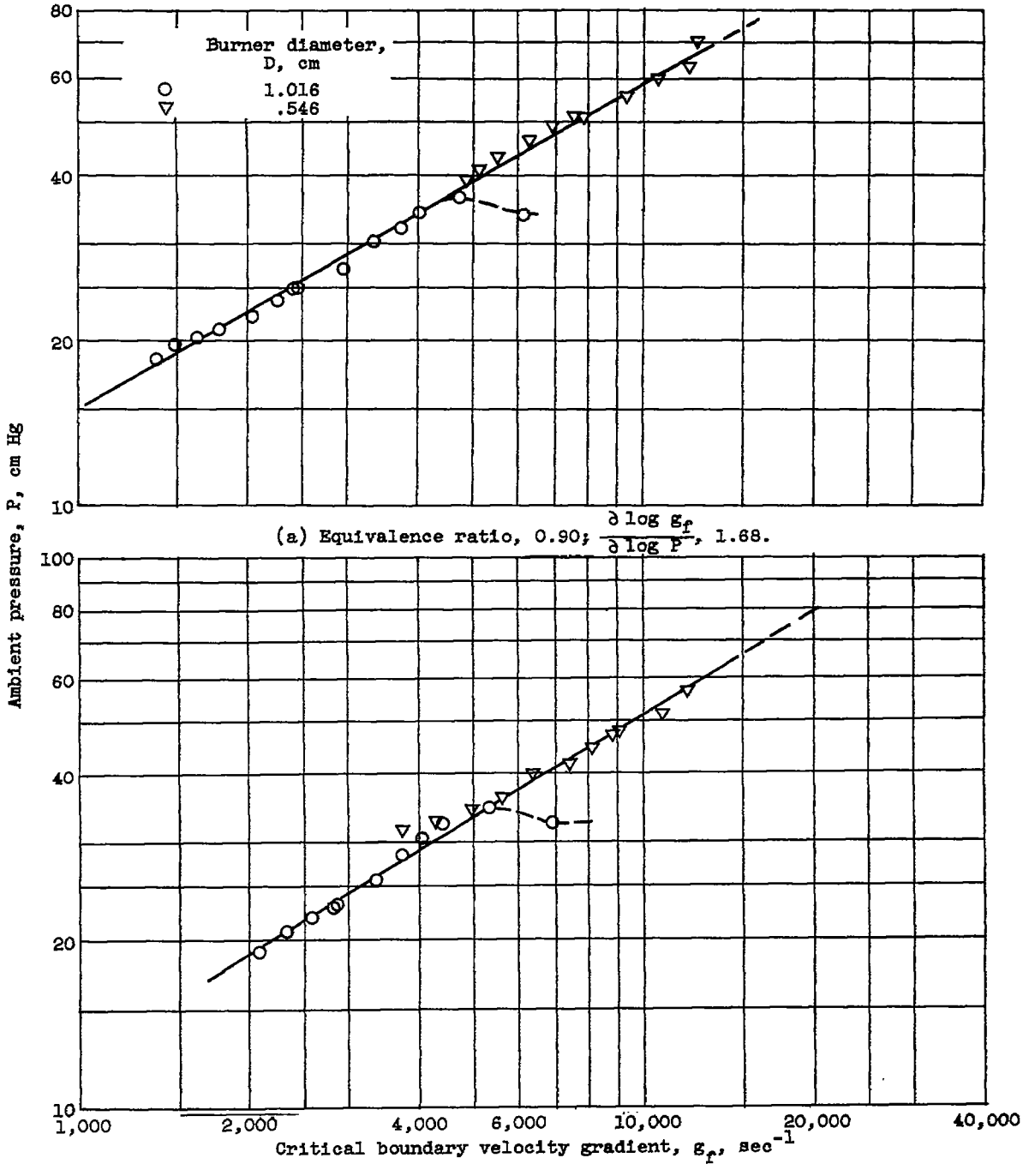

(a) Equivalence ratio, 0.90; $\frac{\partial \log g_f}{\partial \log P}$, 1.68.

(b) Equivalence ratio, 1.10; $\frac{\partial \log g_f}{\partial \log P}$, 1.59.

Figure 11. - Flashback of laminar hydrogen-argon-"air" flames.

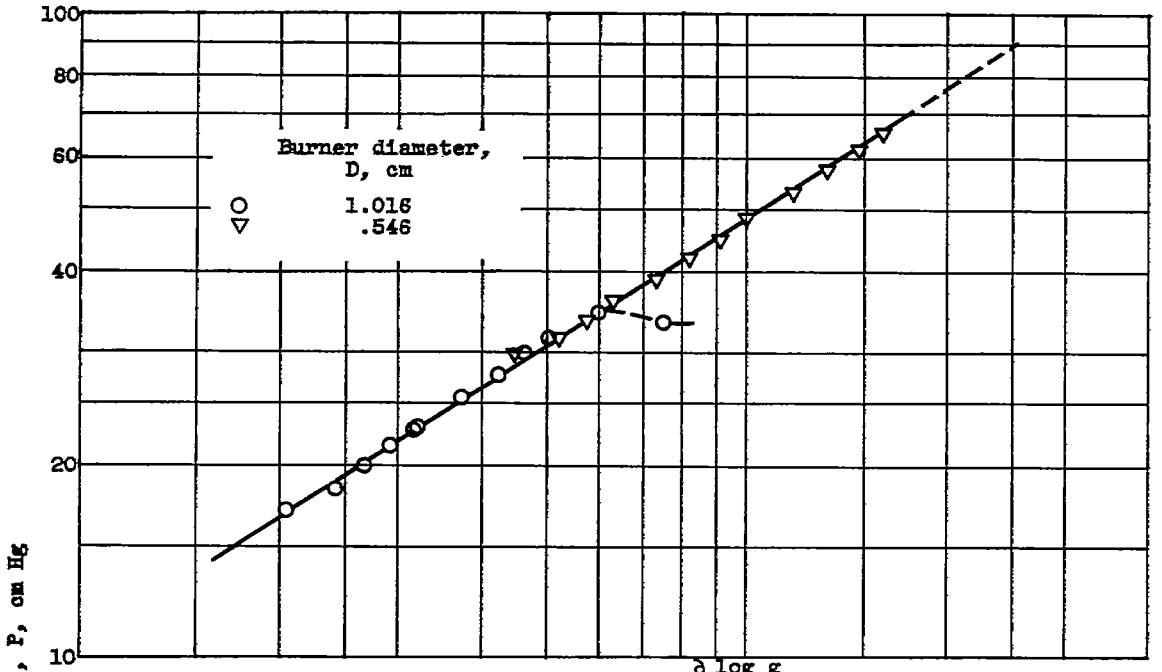

(c) Equivalence ratio, 1.50; $\frac{\partial \log g_f}{\partial \log P}$, 1.49.

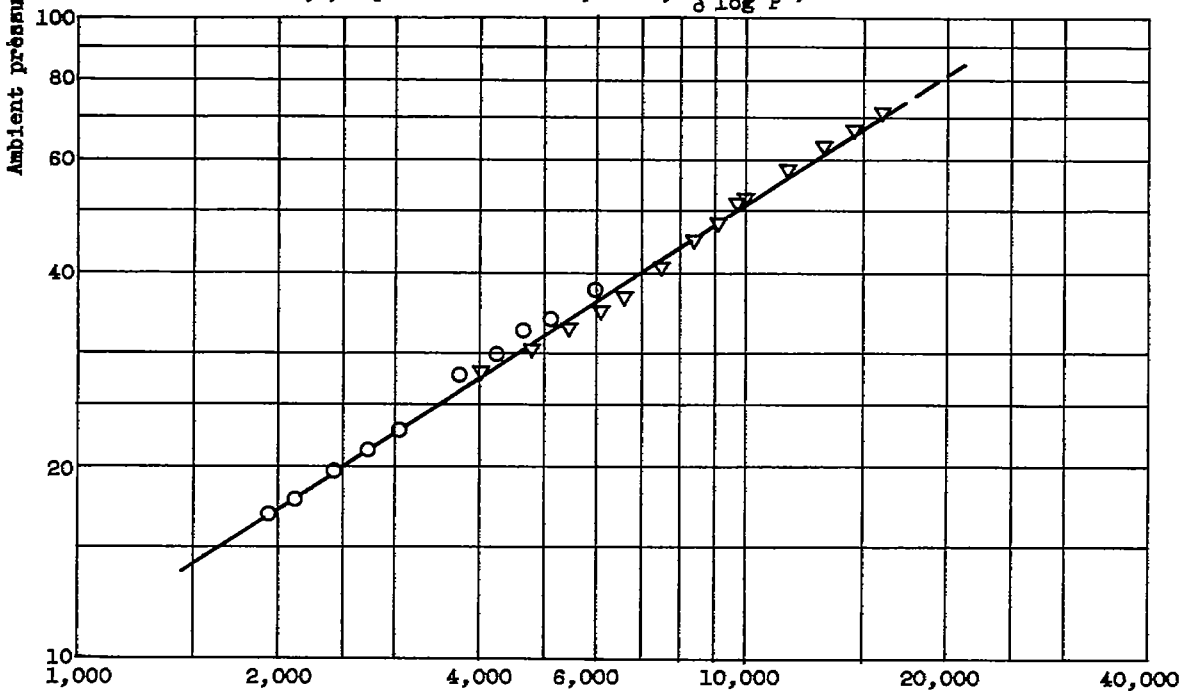

(d) Equivalence ratio, 1.80; $\frac{\partial \log g_f}{\partial \log P}$, 1.49.

Figure 11. - Continued. Flashback of laminar hydrogen-argon-"air" flames.

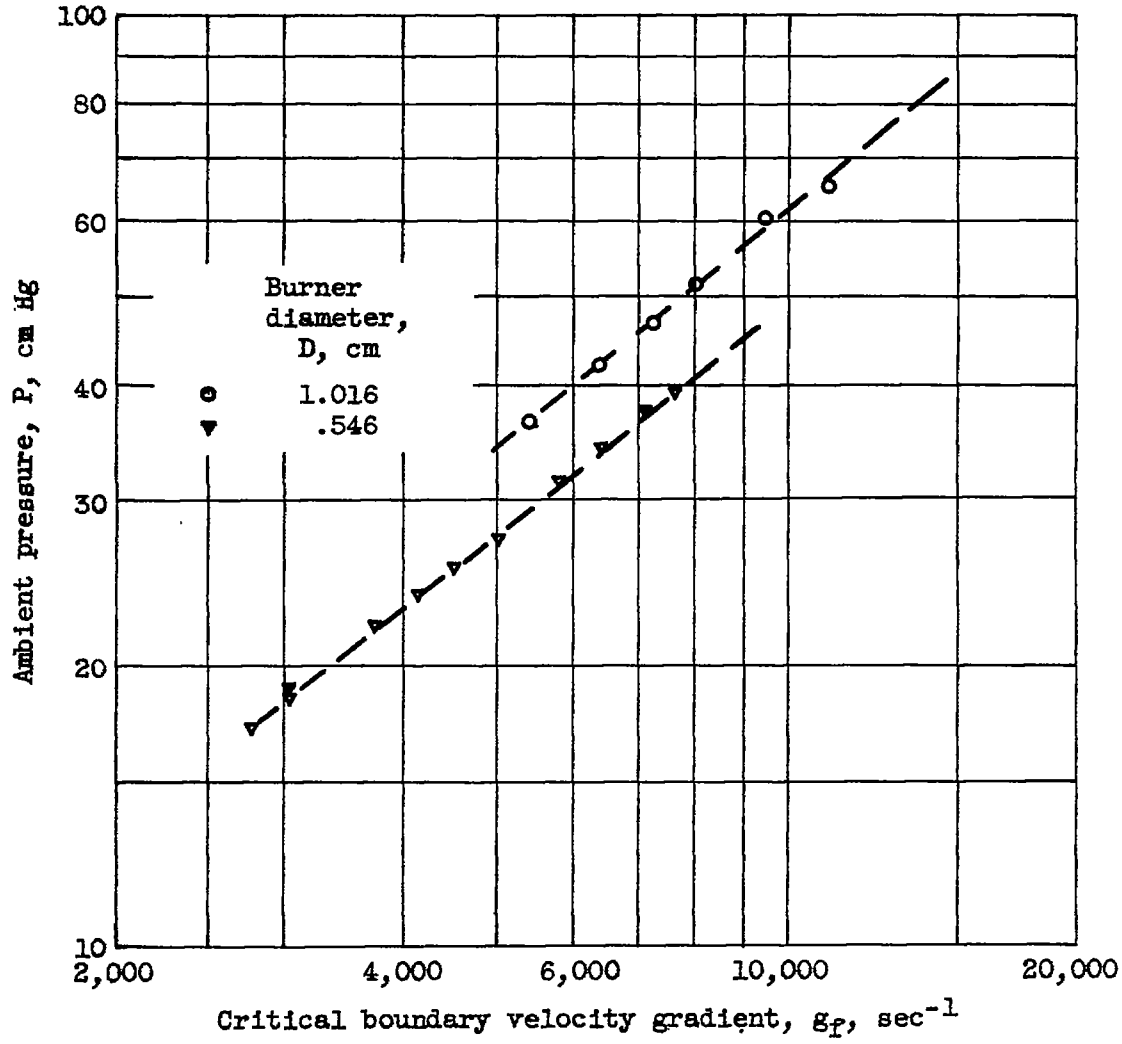

(e) Equivalence ratio, 2.25; $\frac{\partial \log g_f}{\partial \log P}$, 1.22.

Figure 11. - Concluded. Flashback of laminar hydrogen-argon-"air" flames.

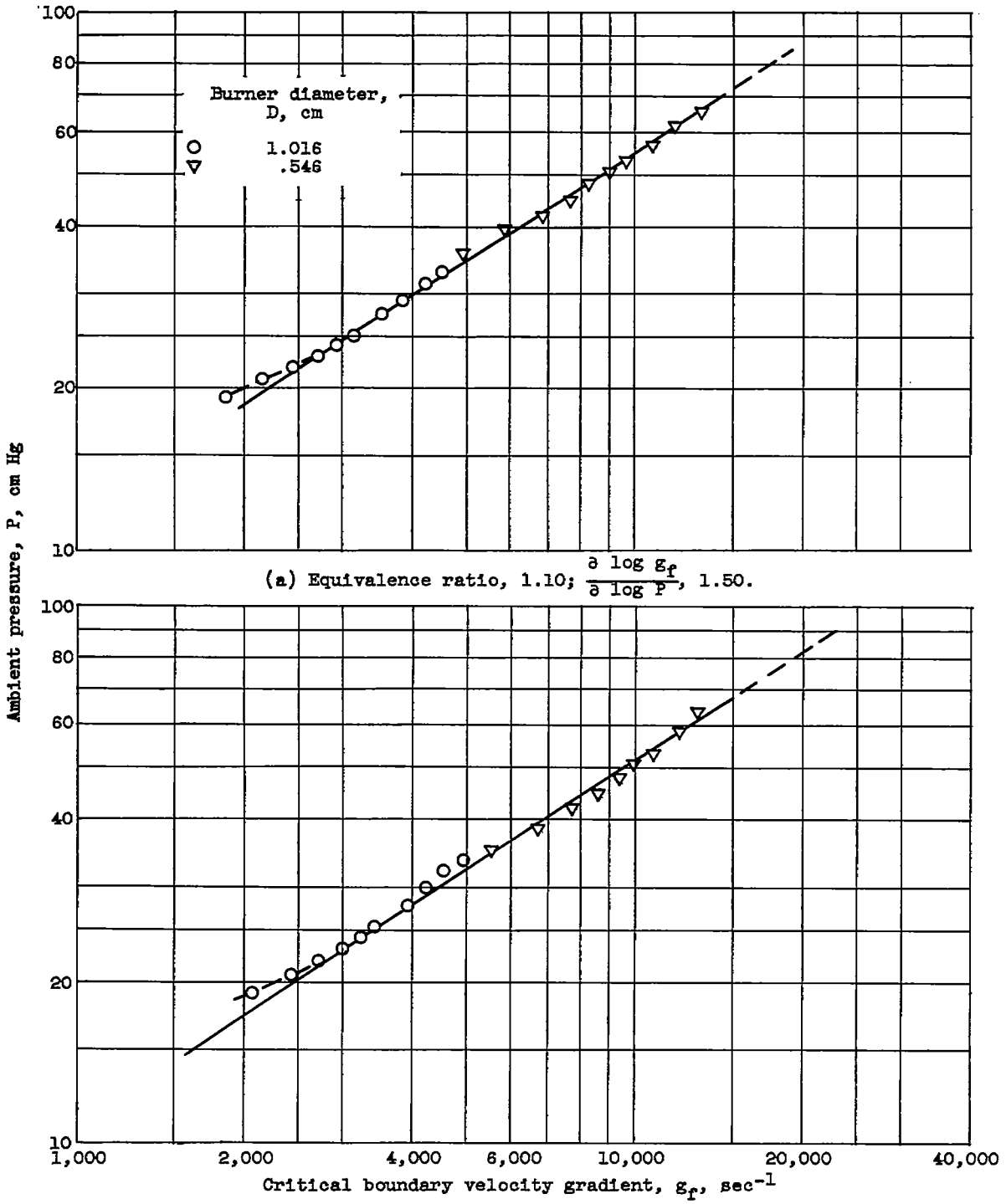

(a) Equivalence ratio, 1.10; $\frac{\partial \log g_f}{\partial \log P}$, 1.50.

(b) Equivalence ratio, 1.50; $\frac{\partial \log g_f}{\partial \log P}$, 1.48.

Figure 12. - Flashback of laminar hydrogen-helium-"air" flames.

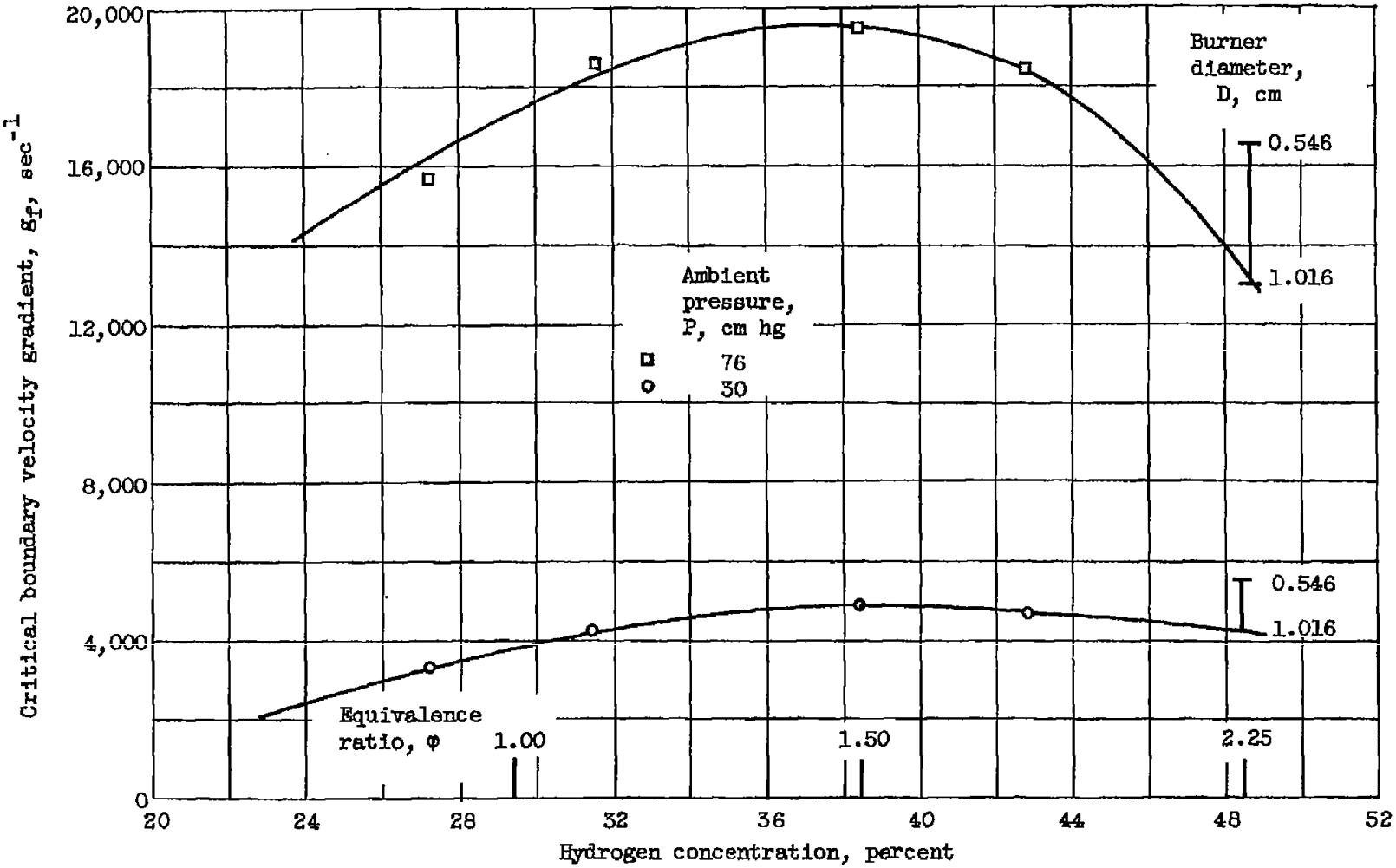

Figure 13. - Flashback critical boundary velocity gradient as function of composition for laminar hydrogen-argon-"air" flames.

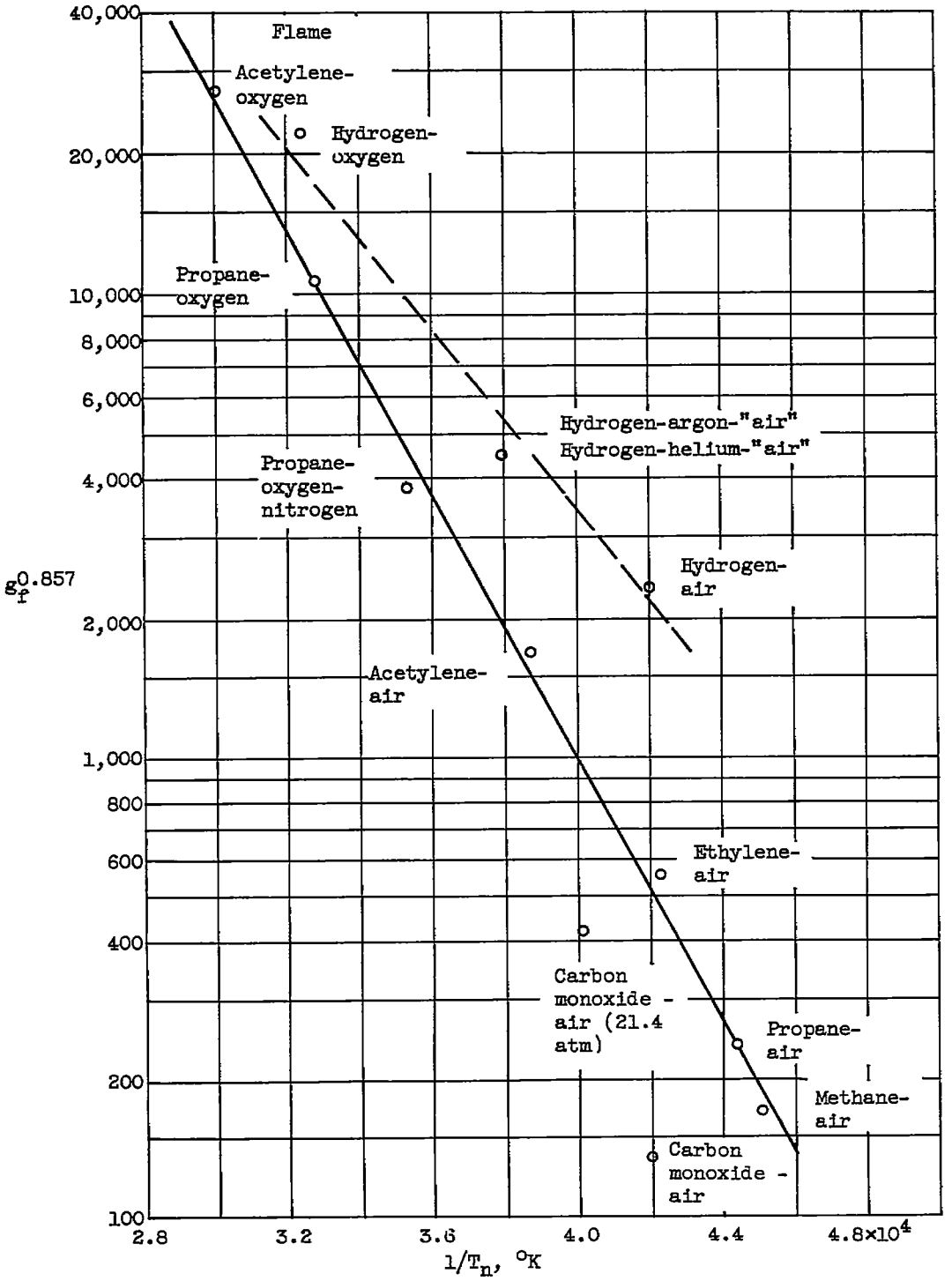

Figure 14. - Stoichiometric critical boundary velocity gradient as function of adiabatic flame temperature.